THE ASTROPHYSICAL JOURNAL

AN INTERNATIONAL REVIEW OF SPECTROSCOPY AND ASTRONOMICAL PHYSICS

VOLUME 88 DECEMBER 1938 NUMBER 5

ON THE FREQUENCY OF SUPERNOVAE

F. ZWICKY

ABSTRACT

In the period from September 6, 1936, to January 31, 1938, some three thousand nebulae brighter than apparent magnitude $m=15$ were systematically searched for supernovae. Each nebula appears, on the average, on about seven photographs taken at intervals spaced not closer than one month. This search is equivalent to the continuous control during one year of about eighteen hundred nebulae. Since three supernovae were found in the period mentioned, it follows from our present data that the average frequency of occurrence of supernovae is about one supernova per extragalactic nebula per six hundred years.

Several years ago Baade and I called attention to the occasional occurrence in extragalactic nebulae of temporary stars[1,2] whose brightness at maximum exceeds that of ordinary novae by about a factor of 1000. In some respects these new temporary stars behave like giant analogues of the ordinary novae. For instance, the light-curves of the two types of stars are of a similar character. In conformity with this conclusion, we proposed to call the new class of stars "supernovae," a designation which at the present time seems to have been generally adopted in the astronomical literature. It should be emphasized again, however, as Baade and I did previously, that there exist not only qualitative similarities but also qualitative

[1] W. Baade and F. Zwicky, *Phys. Rev.*, **45**, 138, 1934, and **46**, 76, 1934; *Proc. Nat. Acad. Sci.*, **20**, 254, 1934. See also F. J. M. Stratton, *Handbuch d. Astrophysik*, **7**, 671, 1936.

[2] F. Zwicky, *Scientific Monthly*, **40**, 461, 1935; *Proc. Nat. Acad. Sci.*, **22**, 457, 1936, and **22**, 557, 1936; *Pub. A.S.P.*, **48**, 191, 1936, and **49**, 204, 1937.

differences between supernovae and novae and that the analogies between the two classes of temporary stars cannot be driven too far. In particular, it would seem that the physical causes for the two types of nova outbursts are different in character.

From the analysis of data available on supernovae recorded in the past, we concluded that the discovery and the systematic investigation of these rare objects promises to throw much light on a number of fundamental problems of physics and astronomy. We therefore worked out a general program which contemplates a determined search for supernovae as well as their subsequent observational and theoretical investigation. One part of this program called for the construction of powerful wide-angle telescopes permitting the photography of large areas of the sky with great speed and uniformity. We are greatly indebted to Drs. John A. Anderson and R. A. Millikan to whose sympathy and support for our project it is mainly due that the construction of an 18-inch F/2 Schmidt telescope, to be located on Palomar Mountain, was decided upon by the Observatory Council of the California Institute of Technology.

The mentioned Schmidt telescope was completed in the fall of 1936 and put into operation on September 5 of the same year. Since that date this telescope has been mainly used to search for supernovae.

Thus far on Palomar Mountain three supernovae have been found in the extragalactic systems NGC 4157, 1003 and IC 4182, respectively. In December, 1937, I located a fourth and definitely variable object near the northwest edge of the southern nebula NGC 1482. Because of bad weather conditions, as well as some additional unfortunate circumstances, no spectrum of this object was obtained. and it will be necessary to wait until next fall before it can be ascertained whether or not it is another supernova.

The subject of the following lines is the discussion of the frequency of occurrence of supernovae in an average nebula. The statistical considerations involved are based on the data obtained in the search for supernovae with the Schmidt telescope alone. This is by far the most uniform set of data available at the present time. The time interval underlying our calculations is arbitrarily limited to the period from September 5, 1936, to January 31, 1938.

A. NEBULAR FIELDS HELD UNDER CONTROL

The choice of the nebular fields to be searched for supernovae was guided by the following considerations: (1) to detect as many supernovae as possible in order to obtain statistical data regarding the frequency of occurrence of supernovae in average nebulae as well as the dependence of this frequency on individual nebular types and (2) to discover supernovae of great apparent brightness which lend themselves to detailed spectroscopic investigations and which can be followed with the great telescopes over long intervals of time. To accomplish these two goals the following types of fields were chosen.

a) In the first place, it was obviously advisable to photograph as often as possible those clusters of nebulae which can be comfortably reached with the Schmidt telescope. This includes, before all, the Virgo cluster of nebulae as well as its northern and southern extensions into Coma Berenices, Canes Venatici, Ursa Major and Hydra and Centaurus, respectively. Occasionally, but much less frequently, the Andromeda-Pisces-Perseus cloud of nebulae, the Pegasus cluster, and the Cancer cluster were also searched.

b) Second, special emphasis was to be laid on all the bright near-by systems such as the great nebula in Andromeda, M 33, 51, 81, 82, 101 and NGC 55, 247, 253, 2403, 4945, 5128, 5236, etc.

In discussions with Dr. Baade, it was also decided to hunt for and to hold under control as many as possible of the near-by faint but resolvable nebulae of the type of IC 342 and 1613. Several dozen of these nebulae of low surface brightness were located and frequently photographed—a move which proved to be a fortunate one, since, as a result, the absolutely brightest of all supernovae was found in a nebula of this type (IC 4182). Baade has been engaged for some time in photographing nebulae of this type under the best conditions of seeing in order to determine the distances of these objects from the apparent magnitudes of the brightest stars which they contain. For instance, Baade had already determined the absolute distance of IC 4182 in 1936, and he was consequently able to calculate immediately after its discovery the absolute brightness of the supernova which appeared in this nebula in August, 1937. Furthermore, internal obscuration is practically negligible in open

and faint nebulae of the type of IC 1613 and 4182. The determination of the absolute brightness of supernovae which appear in such systems is not, therefore, incumbered by any serious uncertainties because of obscuration effects.

The main purpose of covering fields of type *a* which contain rich clusters of nebulae is to increase the probability of finding supernovae and to obtain data of their frequency of occurrence with a minimum number of exposures. Any individual supernova, however, will furnish the most information if it flares up in a nebula of class *b*. Since these latter nebulae are among the nearest to us, novae appearing in them will be, on the average, those of the greatest apparent brightness. The distances of nebulae in class *b* can usually be determined with considerable accuracy, so that the absolute brightness of supernovae in these systems may be calculated. Also, some nebulae of class *b* are near enough so that both common novae and supernovae which belong to them are observable with the great telescopes—a fact which allows an accurate comparison of the frequency of occurrence as well as of the intrinsic characteristics of these two types of temporary stars.

At the present time about 150 different nebular fields are searched with the Schmidt telescope in the course of a year. These fields cover approximately one-fifth of the entire sky visible from Palomar Mountain. The distribution of these fields over the sky is shown in Figure 1.

The extended uncontrolled areas roughly outline those parts of the sky which are occupied by the Milky Way.

The circular field actually used in the Schmidt telescope has a diameter of about 9.5 degrees and covers approximately 70 square degrees. Each field is schematically shown as a circle in Figure 1. However, in the representation used, the circles must be thought of as stretched parallel to the right-ascension axis by factors $1/\cos\delta$, whereas the dimensions along the declination axis δ are those of the actual fields.

The following statistical considerations are based on the control of 122 fields which form a part of the 150 fields shown in the figure which are controlled at the present time. On these fields, about 3000 different nebulae of apparent magnitudes brighter than $m = 15$ were

marked and systematically searched for supernovae. It is assumed that these nebulae form a representative sample collection of the nebular content of that part of the universe which can at the present time be explored with the largest telescopes. Our search for temporary stars in the sample collection of nebulae chosen is limited to objects which at their maximum brightness have an apparent magnitude $m < 16.5$. Fainter objects would almost certainly have escaped my attention. The faintest supernova which I have found thus far appeared in NGC 4157. It had an apparent magnitude $m = 16.3$ at the time of discovery.

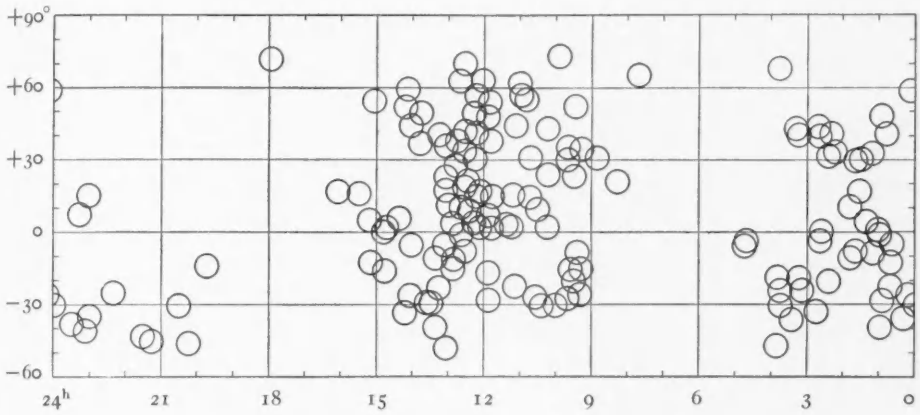

FIG. 1.—Distribution of fields controlled in the supernova search

The controlled fields include about 700 nebulae brighter than $m = 13$. Most of these nebulae are listed in the Shapley-Ames catalogue of nebulae, in which 1250 objects brighter than the thirteenth magnitude are given. Among the three supernovae which I have found, only the one in NGC 4157 flared up in a nebula of the Shapley-Ames list. The two remaining ones appeared in NGC 1003 and IC 4182—nebulae which are somewhat fainter than $m = 13$.

Circumpolar fields were photographed throughout the year when weather conditions permitted it. The most southern nebulae could be controlled each year during a few months only. Most photographs were at least superficially searched immediately on the day after the exposures were taken in order to insure the early discovery

of supernovae. This procedure, combined with the kind co-operation of Mount Wilson astronomers, enabled us to secure early spectra of the newly discovered objects.

The standard exposure time for the pictures taken is thirty minutes. With a clear and moonless sky the resulting photographs show stars of apparent magnitude $m = 17.5$. Only good pictures have been made use of in our analysis.

B. THE FREQUENCY OF SUPERNOVAE AS DEDUCED FROM THE DATA OBTAINED WITH THE SCHMIDT TELESCOPE

We assume that any supernova would have been discovered in a given nebula if it had made its first observable appearance not longer than one month in advance of any date at which this nebula was photographed. According to our present knowledge of the light-curves of supernovae, this assumption is, on the average, definitely too pessimistic if the nebula in question is brighter than about $m = 14$. On the other hand, the said assumption is on the average too optimistic in the case of those nebulae under our control, the brightness of which is fainter than $m = 14$. The resulting partial overestimates and underestimates of the frequency of supernovae, however, approximately balance each other.[3] The final result ar-

[3] The casual reader might here ask how it is at all possible to overestimate the frequency of supernovae since one certainly cannot discover more supernovae than actually occur. The overestimates of the frequency are a result of the necessarily schematic mode of calculation used in this paper. The following hypothetical case perhaps best illustrates how an overestimate of the frequency results.

Suppose, for the sake of argument, that in the Andromeda nebula supernovae occur, on the average, once every thousand years. The apparent brightness of such supernovae at maximum will lie in the approximate range of magnitudes $5.4 < m < 11.6$, and their lifetime as stars of apparent magnitude $m \leq 17.5$ (limiting magnitude of the Schmidt telescope) will be longer than six months. If, therefore, we photograph the Andromeda nebula for n thousand years once exactly every six months, we shall not miss any supernova, i.e., we shall find n supernovae, provided n is large enough to make statistical fluctuations negligible. According to our mode of calculation, the control value of our hypothetical search will be equal to the number, $2000 \times n$, of photographs, multiplied by the control value of each photograph, which we have set equal to one month. The total control value of our search, therefore, is $2000 \times n$ nebula months, or $1000 \times n/6$ nebula years. Dividing this number by the number n of supernovae found, we arrive at a period of $1000/6 = 133$ years, during which, according to our calculation, we should on the average find one supernova in the Andromeda nebula. Our calculation thus results in a sixfold overestimate of the actual

rived at in this paper is, consequently, fairly trustworthy, with some possible reservations to be mentioned later.

In order to be able to express ourselves briefly, we now introduce the idea of a control month per nebula which we shall also call a "nebula month." Suppose that we have at our disposal a good standard exposure of a given nebula taken at a certain date. If the same nebula is photographed at a later date, not less than one month after the first date, we assume, in keeping with the preceding considerations, that we have controlled the said nebula for one month as far as the appearance of supernovae in this nebula is concerned. If n photographs of a given nebula are available at intervals not spaced more closely than one month, this set of photographs corresponds to n nebula months of our supernova control. Twelve control months are equivalent to a control year per nebula, or a nebula year. It is obvious that the value of a given nebula month depends somewhat on the number of pictures taken of the nebula in question during the month. With the exception of some of the near-by nebulae, time has, however, been lacking to cover the majority of our fields more often than once a month.

In the period from September 5, 1936, to January 31, 1938, we have obtained in all 611 good photographs, which are distributed more or less uniformly over the 122 fields held under control. If a given field which covers N marked and controlled nebulae is photographed n times at intervals spaced less closely than one month, we register the result as nN nebula months. The sum of all the products nN for all the controlled fields is the total number of nebula months. For our search this sum total is

$$\sum nN = 22{,}037 \text{ nebula months}, \qquad (1)$$

---

frequency of supernovae in the Andromeda nebula. It is obvious that we should have arrived at the correct frequency of one supernova per thousand years if we had adopted six months instead of one month as the control value of each photograph.

From the preceding considerations it is also clear that our method of calculating the frequency of supernovae would not result in any overestimates of this frequency for the near-by nebulae if we could photograph all these nebulae once every month. Because of the position in the sky of many of these nebulae, and also because of the interference of periods of bad weather as well as other fortuitous circumstances, such a program, unfortunately, cannot be carried out.

which is equivalent to 22,037 control months for any individual average nebula. Expressed in terms of years, our search corresponds to $Y = 22{,}037/12 = 1836$ control years or nebula years.

Three supernovae were found in our sample collection of nebulae during the search whose controlling value we just found to be equal to 1836 nebula years. Disregarding statistical fluctuations, we identify the observed number of three supernovae with the number of supernovae to be expected in an average nebula during 1836 years. As a first approximation, we therefore arrive at the result that in an average nebula supernovae may be expected to flare up at a rate of one in

$$\nu = \frac{1836}{3} = 612 \text{ years} . \qquad (2)$$

This result substantiates the essential correctness of the original estimate of the frequency of supernovae which Baade and I communicated in our first papers on supernovae.[1] The present result, however, is based on a set of observations which is far more uniform and reliable than the meager data which we had at our disposal when we made our first and consciously tentative estimate of the frequency of supernovae.

We may state the result (2) somewhat differently if we go back to equation (1). From the fact that three supernovae were found in a search whose control value is given by (1), it follows that one supernova should be found, on the average, if $22{,}037/3 = 7346$ different nebulae were photographed and compared with standard photographs of the same nebulae taken at sufficiently earlier dates.

It has been estimated that in the Andromeda nebula as well as in our own galaxy about twenty common novae flare up yearly. This frequency of occurrence of ordinary novae in each of these two stellar systems is, therefore, about ten thousand times greater than the frequency of occurrence of supernovae in an average nebula.

The preceding calculations may be supplemented by an estimate of the frequency of supernovae in our sample collection of nebulae of apparent brightness greater than that corresponding to apparent magnitude $m = 13$. As has been mentioned, this partial collection of nebulae now controlled at Palomar contains about seven hundred

objects—a number which would seem to be large enough to make the said collection a representative one. If we denote by N_{13} the number of nebulae on a given field whose apparent magnitude is $m < 13$, then our search represents a sum total of control months for these nebulae, which is given by

$$\sum n N_{13} = 5521 \text{ nebula months}, \tag{3}$$

or $5521/12 = 460$ control years or nebula years. Since only one supernova was found in the partial collection of nebulae for which $m < 13$, we conclude that in the first approximation

$$\nu' = 460 \text{ years} \tag{4}$$

represents the period during which one may expect one supernova to appear in a given individual average nebula of our partial collection.

Since we have dealt in the preceding pages with very small numbers, namely, the appearance in our two controlled collections of nebulae of one and three supernovae, respectively, the difference between the values of ν and ν' is well within the bounds of the probable deviations. The uncertainties inherent in the statistics of small numbers can be only overcome by a prolonged and intensive search for supernovae until ν becomes large enough to make the relative deviation $\nu^{-1/2}$ as small as possible. Although I propose to continue the present program for some time, it is obvious that the accumulation of results will be necessarily slow unless other observers can be induced to co-operate. I am happy to hear from Dr. N. U. Mayall, of the Lick Observatory, that he intends to control the Coma cluster of nebulae with the 36-inch Crossley reflector. Since cluster nebulae are preponderantly of the elliptic type whereas in the general field spirals are the most numerous, the comparison of the frequency of supernovae in cluster nebulae and in nebulae of the general field promises to furnish us with significant data concerning the stellar content of different types of nebulae. In other words, if the probability for a given star to become a supernova depends on the type of this star, as would seem to be likely, the frequency of

occurrence of supernovae in different types of nebulae will furnish us information regarding the frequency of potential supernovae as a function of nebular type. In the cases of nebulae in which, even with the large telescopes, no individual stars can be seen, the occurrence of supernovae indicates that these nebulae are actually stellar systems. For instance, it has thus far not been possible to resolve globular nebulae into individual stars, and the question has sometimes been raised whether such nebulae are stellar systems at all. The appearance of a supernova in the globular nebula NGC 4486 in 1919 thus is equivalent to a first step toward the proof that nebulae of the globular type are composed of stars. A similar conclusion may be reached about the nebula NGC 5253 from the appearance in it of the supernova known as Z Centauri. Furthermore, the search for supernovae with telescopes of much greater focal length than that of our Schmidt telescope (36 in.) is of interest for the following reason. On our photographs the scale is so small (1° = 16 mm) that elliptic nebulae as well as the nuclei of spirals appear so black on our standard exposures that the discovery of supernovae near the center of these nebulae is difficult, if not impossible, unless the time-consuming procedure were adopted to secure for every controlled field several simultaneous photographs with widely varying exposure times. Photographs on a much larger scale, taken with telescopes of longer focal length, would obviously be helpful to clear up the question of the frequency of supernovae in the concentrated parts of nebulae. As far as my present search is concerned, no guaranty can be given that no supernova has been missed which may have appeared in a dense central region of one of the controlled nebulae.

In addition to the difficulties just mentioned, the personal equation in the search for supernovae must be considered. Although I have searched each film once immediately, and a few days later very thoroughly for a second time, no other observer has so far controlled my search. I have tried, as far as possible, to eliminate the resulting uncertainty by re-examining all old photographs at a much later date. This I have done systematically by using successive previous exposures as standards with which the most recent exposures are compared. However, this system of self-control by successive cross-

comparison must be continued for a much longer time before it will be possible to state with any certainty that no supernova has been missed.

C. DEGREE OF COMPLETENESS OF OUR SEARCH

According to Hubble,[4] the average number N_m of nebulae brighter than the apparent magnitude m, per square degree, is given by

$$\log N_m = 0.6m - 9.1 . \tag{5}$$

For $m = 15$ we have $N_m = 0.8$. Discounting the cap around the south pole from the declination $\delta = -50^\circ$ to $\delta = -90^\circ$, as well as the zone of avoidance along the Milky Way in which no nebulae are seen, approximately 15,000 square degrees remain. The entire unobscured, or only partially obscured, part of the sky seen from Palomar therefore contains about $15{,}000 \times 0.8 = 12{,}000$ nebulae whose apparent magnitudes satisfy the inequality $m < 15$. Of these nebulae about 3000, or one-fourth of all, are controlled in our search for supernovae. Presumably not all supernovae are detected which flare up in the controlled nebulae. This is mainly due to four circumstances, some of which have already been touched upon in the preceding pages. We recapitulate: (1) Intrinsically faint supernovae in the most distant nebulae of our controlled collection will be missed. (2) The personal equation enters, inasmuch as only a single observer has so far searched the plates. (3) Relatively faint supernovae which appear in concentrated elliptic nebulae or near the extremely bright nuclei of spirals may be missed because of the small scale of the photographs taken with the Schmidt telescope. (4) Decimation of the apparent brightness of supernovae because of internal obscuration in the nebulae in which they appear further increases the probability that some supernovae, especially in the distant nebulae, are missed.

The difficulties listed under 2 and 3 may be overcome by the methods already discussed. The difficulties listed under 1 and 4 may be overcome only through the use of more powerful telescopes if a given sample collection of nebulae is adhered to, or through the

[4] E. Hubble, *The Realm of Nebulae*, p. 71, Yale University Press, 1936.

restriction of the search with the Schmidt telescope to nebulae whose distances are sufficiently small.

The average absolute photographic magnitude of supernovae, according to Baade, is

$$\overline{M}_s = -14.2\,, \tag{6}$$

with a dispersion of about 1 mag. Assuming, as we did, that we can detect every supernova whose apparent magnitude is $m \leqslant 16.5$, an intrinsically faint supernova of the absolute magnitude $M_s = -11$ will be found only if the distance modulus of the nebula in which it appears is

$$m_N - M_N \leq 16.5 + 11 = 27.5\,. \tag{7}$$

For nebulae whose distance moduli satisfy this requirement, our control for supernovae is practically complete. These nebulae, as Baade has pointed out, are exactly those whose distances may be determined with the largest telescopes from the criterion of the brightest stars which they contain, provided they are of the late nebular types.

Just how many supernovae may have been missed in nebulae whose distance moduli are larger than 27.5 can, in principle, be calculated from the now known average magnitudes and dispersion in magnitudes of nebulae and supernovae, combined (in case 4) with some sufficiently well-known data on the internal obscuration in nebulae. This calculation, however, is somewhat lengthy and must for the present be omitted, since it necessitates a fairly accurate determination of the apparent magnitudes of all the fainter nebulae which are included in our controlled collection of nebulae—a task which has not yet been carried out.

The restriction of the supernovae search to nebulae whose control with the 18-inch Schmidt telescope is complete is not practically feasible, because the number of nebulae of this type is too small. Much more complete data on the frequency of occurrence of supernovae will, however, be accumulated in a short period of time with the help of a 48-inch Schmidt telescope, the construction of which has been decided upon by the observatory council of the California

Institute of Technology. This telescope will probably reach stars whose apparent magnitude is as faint as $m = 20.5$. Nebulae brighter than $m = 17$ may then be searched with the expectation that the corresponding control for the appearance of supernovae will be of the same relative completeness as the search for supernovae in nebulae brighter than $m = 15$ with the 18-inch Schmidt telescope. The average number N_{17} of nebulae per square degree whose $m \leq 17$ according to the relation (5) is given by

$$N_{17} = 12.6 . \tag{8}$$

On a plate covering 100 square degrees, about 1260 nebulae brighter than $m = 17$ may be expected. On plates which include rich clusters, at least 2000 nebulae whose $m \leq 17$ will be included. On ten such plates, 20,000 suitable nebular images may be controlled for the appearance of supernovae, with the hope that about ten to twenty supernovae will be found during one year—a number which is sufficiently high to reduce very quickly every type of statistical fluctuation.

In the taking of the photographs I have been partly assisted by Dr. J. J. Johnson, of the California Institute of Technology. It is a great pleasure to acknowledge my indebtedness to him for his careful work. The supernova in IC 4182 appeared first on a photograph taken by him on August 25, 1937, on which photograph I found the nova three days later. The two other supernovae in NGC 4157 and NGC 1003 I found on the day after I had photographed the respective fields. That no time was lost in turning the large telescopes of the Mount Wilson Observatory on the newly discovered objects is due to the efficient and immediate co-operation of Drs. Baade, Humason, and Minkowski. Thanks are also due to Dr. Sinclair Smith, who helped to adjust the telescope, and to Mr. Russell W. Porter, who, with inimitable skill, has constructed and supplied us with many useful auxiliary gadgets which have greatly facilitated our work.

California Institute of Technology
Pasadena, California
July 1938

A SIMPLIFIED SPECTROHELIOSCOPE*

G. A. MITCHELL

ABSTRACT

The article describes the construction of a rotating-disk spectrohelioscope provided with two or three sets of slits of different width and an adjustable shutter which permits a choice of slit width without stopping the disk. A device for eliminating inclination of the spectrum lines is also provided. The modified design is such that all the mechanical work except that on the head plate can be done with a breast drill, file, and a few taps.

This paper describes a modification of the rotating disk-type spectrohelioscope suggested by Dr. George Ellery Hale.[1] At Dr. Hale's suggestion, Mr. Hitchcock constructed such an instrument, which was tried with some success; but certain difficulties were encountered which resulted in its being laid aside in favor of more pressing work. Dr. Hale mentions these difficulties:

> This method, however, has several disadvantages compared with the oscillating bar and pair of single slits, among which the invariable slit-width and spacing and considerable inclination of the lines in certain spectroscopes may be mentioned. If I could afford the time I should nevertheless be inclined to develop it further, perhaps introducing adjustable slits and other changes.

It was in order to see how far the disadvantages mentioned could be overcome that the work here described was undertaken. The advantages to be gained, should it be successful, were considerable. The absence of flicker and of dark lines caused by dust in the slits and the elimination of vibration were rewards enough to warrant the attempt; and it was also hoped that simplification of design and a less expensive construction could be attained. With these thoughts in mind and with rather vague ideas of the difficulties involved, work was started. The endeavor has been so to simplify the spectrohelioscope that the amateur and the semiprofessional could construct, or have constructed at small cost, an instrument with which the solar phenomena could be observed with satisfaction.

Since Hitchcock had found a lacquer-coated glass disk to be satis-

* *Contributions from the Mount Wilson Observatory, Carnegie Institution of Washington*, No. 599.

[1] *Mt. W. Contr.*, No. 388; *Ap. J.*, **70**, 425, 1929.

factory, this form was adopted. The problem of cutting the slits in the disk was solved by considering each pair of opposite slits as one continuous line. Indexing then became of no importance. The only requirements were that the center of each slit across the disk pass through the center of rotation and that the slits of each pair be exactly 180° apart.

The procedure was as follows: An $8\frac{1}{2}$-inch disk of $\frac{1}{4}$-inch plate glass, with its front surface coated with black lacquer, was mounted on a shaft. A collet with a hole the size of the shaft was placed in a milling-machine dividing head set with its axis vertical. A swinging arm to carry the cutter was mounted on the milling machine arbor. First a pencil was placed in the swinging arm and indexing was done with the dividing head. Short lines were made halfway round the disk in this manner. Then a cutter was substituted for the pencil over one of the lines in the disk, and a small piece of glass previously coated with lacquer was waxed to the center of the disk. A test line was cut in this piece of glass. The shaft was clamped in the collet with just enough friction to keep it from turning, yet leaving it free enough to be turned in the collet without danger of strain. With the cutter lined up with one of the pencil lines on the side of the disk, the disk was turned 180° and the table traversed longitudinally until the cutter was again central over the same pencil line at the opposite side of the disk. Then a second cut was made on the central piece of glass. The test piece was then removed and examined with a magnifier to see if the two test lines coincided. If not, the distance between them was measured and the table cross-fed half that distance. A second check then determined whether the cutting tool was accurately centered on the axis of rotation of the disk. Then a line was cut clear across the face of the disk, the cutter being raised to pass over the center hub. The remaining slits of the given width were cut by turning the disk against the friction and indexing to the successive pencil lines. This procedure has been found to work very well since it eliminates any error of runout in the bearing of the dividing head or in the collet.

Owing to the wide range of light-intensity of the sun's disk and limb, variable widths of slits are essential for satisfactory observation. Sufficient variation was obtained by making three series of

slits of different widths and arranging a shutter to close those not in use. Three widths were then available for use at will without stopping the instrument. Several shutter arrangements for this purpose are well known; the one adopted and found satisfactory is as follows:

The shaft carrying the disk is hollow, and its rear end, for a sufficient length, is made square. A second shaft, carrying the shutter, is mounted inside the disk shaft; its rear end is also made square but of spiral form and smaller in diameter. A double nut is made in a tube, the front end of which fits the large straight square while the rear end fits the smaller square spiral. By moving this nut longitudinally the shutter shaft is caused to rotate relatively to the outer shaft. By arranging a sleeve to carry the nut and at the same time allow it to rotate, and by mounting on the sleeve a section of rack meshing with a small pinion, the nut may be moved longitudinally during rotation.

In the present instrument a second shutter was placed over the first and set before starting the instrument. The purpose of this second shutter was to close each alternate slit of the series used, thereby gaining a larger field but at a sacrifice of half of the illumination. With the aid of this shutter a field $\frac{3}{4} \times 1$ inch is possible; without it, a field $\frac{3}{8} \times 1$ inch is available. This size seems ample, and the second shutter is of doubtful value. Further, in the present instrument, the three series of forty-eight slits are approximately 0.003, 0.0045, and 0.007 inch wide. Practice has shown that with this type the 0.003-inch slits are too narrow. In the future these slits will be eliminated, thereby gaining more slits to the set and more illumination; or a set of 0.010-inch slits may be substituted.

After the disk had been completed it was found that the inclination of the *Hα* line was a serious detriment which would have to be overcome before the foregoing improvements could be used.

In the disk type of instrument it is necessary that the two light-beams between the two slits and the two concave mirrors be parallel. The following method of correcting the inclination of the spectral line was adopted. Behind each slit-window a 1° prism was mounted, one base down, the other base up. These are common ophthalmic exercise prisms. Behind each of these prisms, similar prisms were mounted with their bases respectively opposite and so arranged as to

PLATE XXI

a

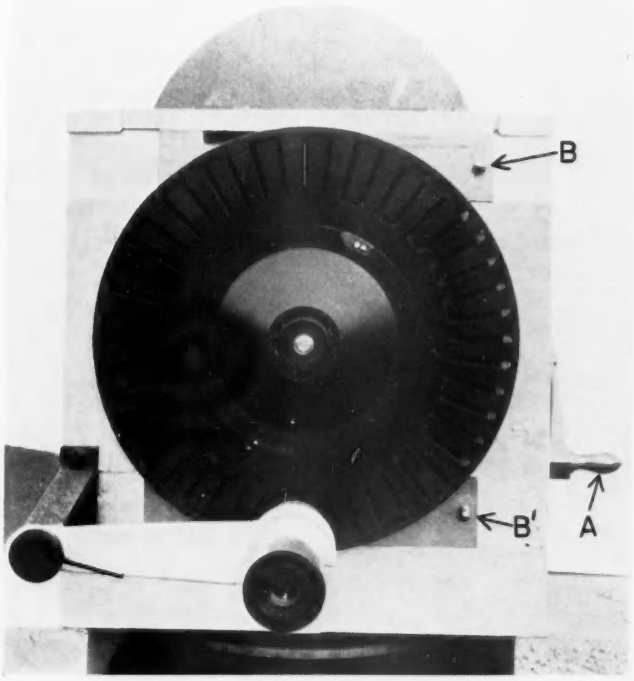

b

ROTATING-DISK SPECTROHELIOSCOPE

a) Front view of head *b*) Slits ruled on disk

UNIV. OF MICH.

PLATE XXII

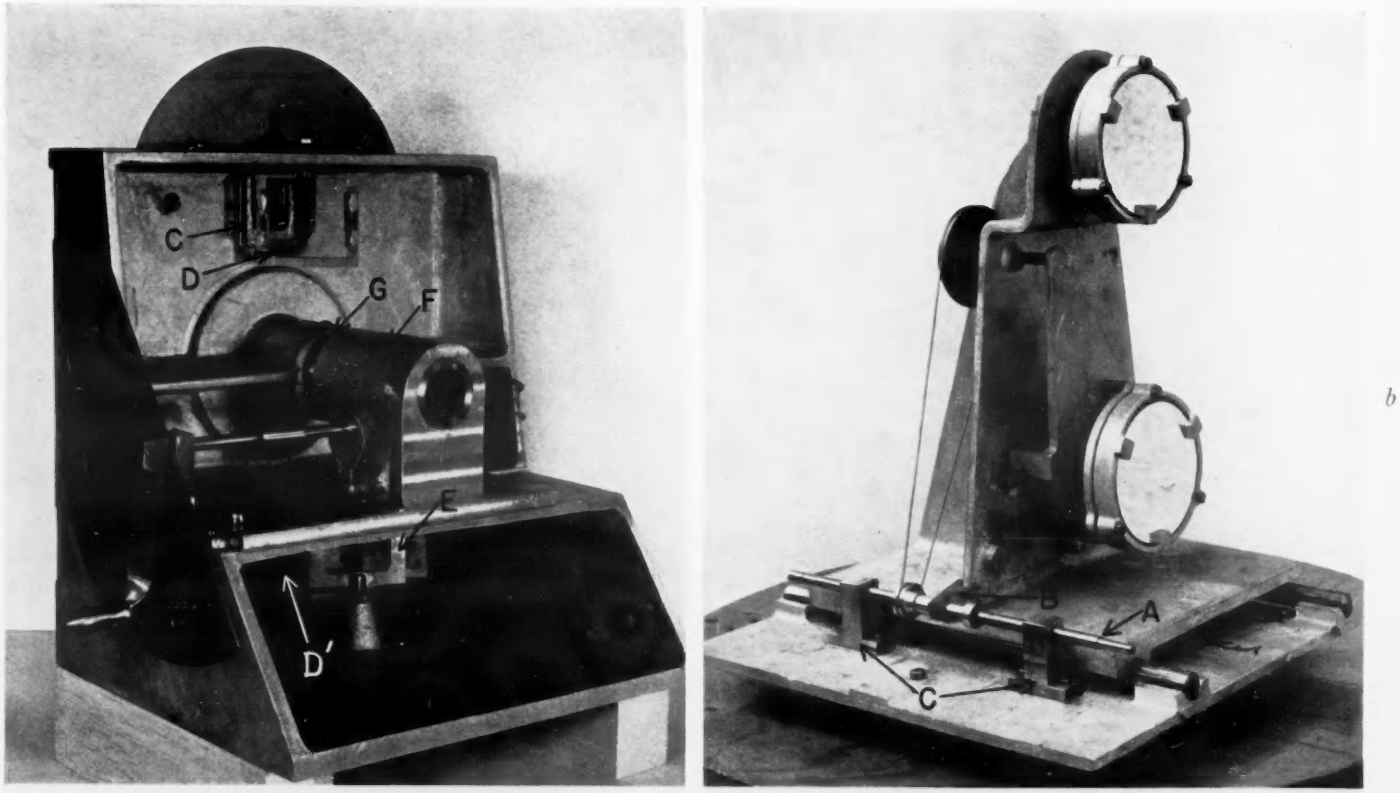

a

b

ROTATING-DISK SPECTROHELIOSCOPE

a) Rear view of head *b*) Mounting for concave mirrors

UNIV. OF MICH.

rotate about a line from base to apex. Rotation of these prisms caused the spectral line to become parallel with the second slit, while at the same time the beams remained parallel and only slightly deviated in passing through the prisms.

With these provisions the disadvantages mentioned by Dr. Hale were overcome to a practical conclusion. Compromises had to be made, but in each case the gain was greater than the loss. It remained to simplify the design as far as possible.

Plate XXI*a* shows the instrument head with the second shutter set for a $\frac{3}{8}$-inch aperture. The lever handle *A* on the side is for shifting the first shutter to select different slits. *B* and *B′* are slides for restricting the apertures to these widths so that only one slit at a time passes across the aperture.

Plate XXII*a* is a rear view of the head showing the prisms for erecting the spectral line. *C* and *C′* (the latter not visible) are the fixed prisms; *D* and *D′*, movable prisms. *E* is the line shifter described by Dr. Hale. The housing *F* carries the double nut for operating the shutter. A string belt, just visible, drives the disk by a V-pulley at *G*.

Plates XXII*b*, XXIII*a*, and XXIII*b* show the simplified design of the remaining parts of the instrument.

Plate XXII*b* shows the concave-mirror mounting. With castings ready, all the work can be done with a file, breast drill, and a few taps. The only thing requiring care is the tangent screw; it should be a nice fit. The mirrors are mounted in cast cells with a cast plate and suitable padding back of them. The three screws have springs behind the backing plate, which hold the cell together. The lower tilting mirror rests on a short piece of $\frac{3}{8}$-inch rod and a spring holds it down; the *V*'s are all cast, and a little filing makes them good enough. The whole upper carriage rides on two pieces of rod on a three-point bearing. A rod is carried from *A* to the operator's station. Reciprocating the rod focuses the concave mirrors, and turning the rod tilts the lower mirror through the two pulleys and the tangent screw. The driving dog *B* rides free on the carriage and hinges out of the way. The purpose is not to put any strain on the carriage should the slides be out of line. The bosses *C* will be cast integral with the base instead of attached as shown in Plate XXII*b*.

Plate XXIII*a* illustrates the grating mounting which is located close behind the head (Pl. XXII*a*). A lower casting with case *V*'s and caps carries a vertical rod; screws are tightened to a nice friction. Clamped tightly to the vertical rod is the tangent-screw lever. Another casting with cast *V*'s and caps holds the grating itself. This should also be tightened up to a nice friction. Cast straps are provided with bosses for adjusting screws. There is no machine work here other than drilling and tapping holes.

Plate XXIII*b* illustrates the coelostat with its first- and second-flat mountings and the lens-holder. The cast base had *V*'s in which to lay $\frac{1}{2}$-inch cold rolled steel rods for ways. The lens is held in a cast ring by a smaller flanged cast ring attached by three screws. This lens-holder is clamped to two vertical rods, which in turn are clamped to a base having three points of support and sliding freely on two of the rods. Pushing and pulling a rod at the observer's station focuses this lens. The coelostat used is the same as described by Dr. Hale. About one hour's lathe work is required to surface the base of the second-flat mounting, bore the hole, and face the piece which rides frictionally on the base. *A* is a small stock worm and worm wheel similar to the one on the coelostat on this mounting. *B* is a tangent screw. All the other work on this mounting may be done with a file, breast drill, and taps. All the bearings are cast *V*'s with caps. *C* is a piece of tubing $\frac{5}{8}$-inch O.D., $\frac{9}{16}$-inch I.D., set eccentrically with screws on a $\frac{5}{16}$-inch rod and forming a cam which pushes a rod in the vertical tube, tilting the second flat. Three screws, top and bottom, guide this rod centrally. Three control rods from this piece of apparatus carry the controls to the operator's station.

Since the uprights are rods or tubing, it is only necessary to cut these to suit and to change the angle of the coelostat in order to adapt it to any latitude. The coelostat may be mounted on a rocker to accommodate it to any latitude, and it may be driven by an electric-clock motor instead of the spring-drive clock now used.

For those who want an instrument as simple as possible, but lacking nothing in final results, the writer suggests the elimination of the shutter-adjusting mechanism, a simple shutter with thumbscrew holding it in place being substituted. This change will reduce the

PLATE XXIII

a

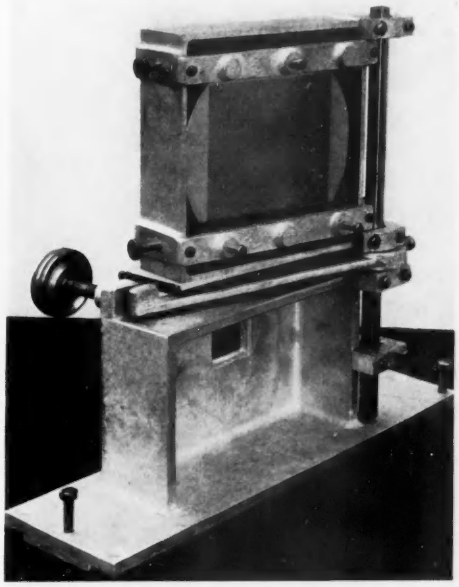

b

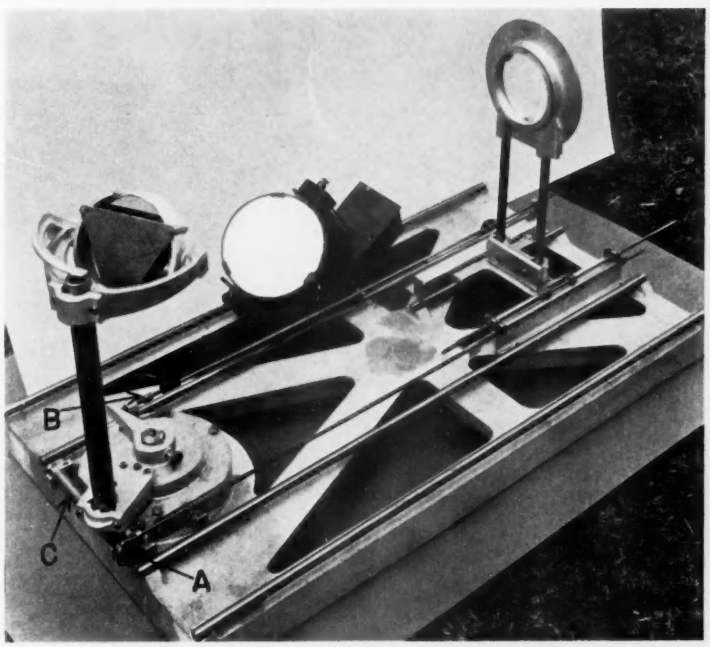

ROTATING-DISK SPECTROHELIOSCOPE

a) Grating mounting *b*) Coelostat and objective mounting

UNIV. OF MICH.

labor of construction a great deal; to change the slit widths it will only be necessary to stop the disk.[2]

For those desiring to build their own outfit completely, detailed instructions are being prepared, covering the full design and each operation of manufacture, together with instructions for operating, and suggesting various simplifications.

In conclusion the writer wishes to thank Mr. Roger Hayward for a suggestion which opened the way for cutting the disk slits easily; Dr. John A. Anderson, for many valuable suggestions; Dr. Rudolf Langer and Mr. Russell W. Porter, for their encouragement; and James T. Barkelew, for help in preparing this article.

CARNEGIE INSTITUTION OF WASHINGTON
MOUNT WILSON OBSERVATORY
July 1938

[2] Arrangements are being made with Messrs. Howell and Sherburne, of Pasadena, to manufacture the complete apparatus. This firm will also furnish the necessary castings at a figure less than the cost of patterns, to those desiring to construct their own instrument. Or they will furnish any part, finished as desired, as well as drawings.

LIMITING MAGNITUDES

FRANK E. ROSS

ABSTRACT

A study has been made of the various optical and photographic factors upon which depends the limiting magnitude which can be reached by any given telescope. The properties of the photographic plate used are of fundamental importance. Of these properties, speed is least important. A formula has been developed for the limiting magnitude which involves the contrast value, and, essentially, the graininess of the photographic plate. Values for these factors have been obtained by laboratory methods for Eastman 40 emulsion, which has been chosen as the best compromise. A large corrective term has been found which depends upon the loss of light in focal images due to scattering effects of various kinds. It has been found possible to compute this loss in any given case with considerable accuracy. Application has been made to three telescopes: the Mount Wilson 60-inch reflector, the Lick 36-inch reflector, and the Yerkes 24-inch reflector.

A study has been made of the effect of pre-exposure in astronomical photography—a field in which there are many conflicting data. A laboratory study of disk images of all sizes shows an unmistakable gain with pre-exposures, a gain which is substantiated by the application of elementary photographic theory. Tests carried out with three different telescopes, however, fail to show any advantage in pre-exposure. An attempt has been made to explain this by a study of the cross-section of stellar images, computed from known optical and photographic data. It was found that the density gradient is the steepest in the case of no pre-exposure. It appears quite probable that this factor is the important one in the discrimination of threshold images.

The value of the brightness of the night sky is fundamental in the problem of limiting magnitudes. A brief account is given of the work done in this field.

I. INTRODUCTION

The present paper is concerned primarily with limiting magnitudes of stars, photographically determined, in so far as they are influenced by optical factors, photographic factors, and sky conditions. It is a truism that no telescope can operate beyond the point where the general sky illumination darkens the background on the photographic plate more than a certain fixed amount measured in photographic density D. This is a fixed amount only for the type of emulsion, the character of development, and the size and character of image. Neglecting losses due to reflection and absorption within the optical train, the specific intensity of the sky brightness at the photographic plate is given by

$$I = \frac{\kappa}{R^2}, \tag{1}$$

where κ is a constant and R is the aperture ratio of the telescope. For a constant or specified limiting density,

$$It^p = \kappa' , \tag{2}$$

in which p is the Schwarzschild exponent. It follows that[1]

$$t^p = \frac{\kappa'}{\kappa} R^2 . \tag{3}$$

Let B_s be the brightness of the sky background, measured in stellar magnitudes per square second. For the moment this may be

TABLE 1

LIMITING MAGNITUDES FOR A GRAINLESS EMULSION

Telescope	Aperture	Focal Length	Diffraction Disk		m_l
	in.	in.		mm	m
Calif. Inst. Tech.	200	667	0".022	0.0018	36.6
Mt. Wilson Obs.	100	508	.045	.0028	35.0
Mt. Wilson Obs.	60	300	.074	.0027	33.9
McDonald Obs.	82	320	.054	.0021	34.6
Lick Crossley	36	210	.124	.0032	32.8
Yerkes Obs.	24	93	0.186	0.0022	31.9

taken equal to 22. Reduced to a circular second, it becomes 22.25. Consider a star of magnitude m having a diameter on the plate of d''. Assume a grainless emulsion having a contrast factor of γ. It will be shown (p. 566) that the following formula applies to this case:

$$m_l = 22.25 - 2.5 \log \left[\frac{(d'')^2}{\text{mod}} \frac{\delta D}{\gamma} \right] , \tag{4}$$

where δD is the minimum contrast recognizable, of the order of 0.01; γ can be taken equal to 6. It is of interest to apply (4) to a number of telescopes. This has been done in Table 1. Seeing and guiding are assumed to be perfect. In the computation of Table 1 the diameter of the diffraction disk, d, in circular measure, is given by

$$d = 1.22 \frac{\lambda}{D} \quad (\lambda = 4500 \text{ A}) .$$

[1] For an application of this formula see p. 568.

It is seen from the table that there is very little variation in the linear size of the diffraction disk for the various telescopes, the diameter being of the order of the size of the individual grains of present-day emulsions. The limiting magnitudes given in the last column are of purely academic interest, being of the order of the unattainable maximum.

Up to the present time very little has been done in pushing exposures to the limiting magnitude. Fast emulsions have been used, which are unsuited, because of their high graininess and low contrast, to the attainment of the faintest limit. Owing to the limitations of time and of patience on the part of the observer, the use of these emulsions is not surprising. The pressing need is of a fast emulsion of low graininess and high contrast. Of the present-day emulsions, probably Eastman 33, corresponding to Seed 23, is the type which represents the best compromise between conflicting requirements. It was with these plates that G. W. Ritchey obtained photographs with the Mount Wilson 60-inch reflector which are difficult to excel.

With photographic and optical equipment as they exist today, the following are pertinent questions to which answer is sought in the present paper:

1. With given optical and photographic equipment, what is the relation between the size of the threshold image and the limiting magnitude obtainable? We know that with improvement in seeing, the size of the threshold image decreases so that, for any given star, the density of its image must increase. At a certain point, however, the effect of increasing density is offset by a reduction in the ability of the observer to discriminate between image and background, because of the grainy structure of the image, so that the increase of efficiency with improvement in seeing must fall off, finally becoming zero or even negative.

2. What modifications must be made in (1) in the important case of exposures pushed to the limit, in which the image is enmeshed in a background of a density which, in general, is of the maximum graininess?

3. What is the photographic density of threshold images as a function of their diameter? The answer furnishes a solution to the

questions raised in (1). For example, it is known that in the case of a large image, a difference in density of 0.01 between image and background is discernible. In the case of a small image, however, having a diameter of the order of 0.10 mm or less, the photographic density has not been measured, so far as the writer is aware.

It will be useful, in evaluating the limiting magnitude which may be obtained under given conditions of size of threshold image and of focal length, to construct a table (Table 2) giving the specific

TABLE 2

VALUES OF B_s

F	d										
	30 μ	40 μ	50 μ	60 μ	70 μ	80 μ	90 μ	100 μ	150 μ	200 μ	300 μ
m	m	m	m	m	m	m	m	m	m	m	m
0.50	16.79	16.16	15.68	15.28	14.95	14.66	14.40	14.17	13.30	12.67	11.79
0.90*	18.06	17.44	16.95	16.56	16.23	15.93	15.68	15.45	14.57	13.95	13.06
1.12†	18.54	17.91	17.43	17.04	16.70	16.41	16.15	15.93	15.04	14.42	13.54
1.25‡	18.78	18.15	17.67	17.28	16.94	16.65	16.39	16.17	15.28	14.66	13.78
2.00	19.80	19.17	18.69	18.30	17.96	17.67	17.41	17.19	16.30	15.68	14.80
3.00	20.68	20.05	19.57	19.18	18.84	18.55	18.29	18.07	17.18	16.56	15.68
4.00	21.30	20.71	20.19	19.80	19.46	19.17	18.91	18.69	17.80	17.18	16.30
6.00	22.18	21.55	21.07	20.68	20.34	20.05	19.79	19.57	18.68	18.06	17.18
8.00	22.81	22.18	21.70	21.31	20.97	20.68	20.42	20.20	19.31	18.69	17.81
10.00	23.29	22.66	22.18	21.79	21.45	21.16	20.90	20.68	19.79	19.17	18.29
12.00	23.69	23.06	22.58	22.19	21.85	21.56	21.30	21.08	20.19	19.57	18.69
15.00	24.17	23.54	23.06	22.67	22.33	22.04	21.78	21.56	20.67	20.05	19.17
20.00	24.70	24.17	23.69	23.30	22.96	22.67	22.41	22.19	21.30	20.68	19.80

* Palomar Schmidt. † Mount Wilson 10-inch, Cook. ‡ Yerkes Bruce 10-inch.

sky brightness B_s as a function of d, the linear diameter of the threshold image, and of F, the focal length of the telescope. It is easy to show that

$$B_s = 22.25 - 5 \log \frac{d}{F \sin 1''}. \qquad (5)$$

It is important to clarify our thought on the meaning of B_s. It means that in a telescope of focal length F, the light of a star of magnitude B_s would equal in intensity the intensity of the sky, provided it were spread over a circular area of linear diameter d. Such a table is basic for the evaluation of limiting magnitudes. For ex-

ample, if it were necessary that the specific intensity of the light of the star, assumed spread over an area of diameter d, be equal to that of the sky background upon which its image is impressed, then the limiting magnitude could be obtained directly from the table, being, in fact, equal to B_s. The present paper is concerned primarily with the corrections which must be applied to B_s to obtain the actual limiting magnitude in any given case.

TABLE 3

RELATIVE EFFICIENCY OF LARGE AND SMALL IMAGES

Mount Wilson 100-Inch					Mount Wilson 60-Inch				
No. of Plates	Diam. of Image		Red. Mag.	R.S.E.	No. of Plates	Diam. of Image		Red. Mag.	R.S.E.
		mm	m				mm	m	
3	0".87	0.054	17.03	51.0	6	1".10	0.040	16.60	76.0
2	1.10	0.069	17.03	32.0	3	1.40	0.052	16.60	45.0
2	1.20	0.075	17.15	24.0	2	1.60	0.059	16.25	48.0
2	1.30	0.081	16.70	31.0	2	1.80	0.066	16.40	33.0
2	1.40	0.087	16.92	22.0	1	2.00	0.074	16.50	24.0
3	1.60	0.100	16.75	19.0	2	2.50	0.092	16.20	20.0
2	1.70	0.106	16.83	16.0	4	2.70	0.099	16.18	18.0
4	2.20	0.137	16.19	17.0	3	10.00	0.370	14.80	4.6
4	3.10	0.194	16.10	9.4	1	18.00	0.660	14.00	3.0
3	6.60	0.413	15.75	2.9	4	35.00	1.290	13.10	1.8
3	14.50	0.906	14.37	2.1	4	55.00	2.020	12.30	1.6
3	30.70	1.920	13.27	1.3	2	75.00	2.760	12.10	1.0
2	48.00	3.000	12.58	1.0					

A large amount of material has been collected by E. P. Hubble[2] on the relation between size of threshold image and limiting magnitude, from observations with the Mount Wilson 100-inch and 60-inch telescopes. The data given in Table 3 have been selected from Hubble's Tables 1*a*, 1*b*, and 1*c*, averages being formed for the sake of conciseness. Eastman 40 plates have been used throughout. The values of the limiting magnitude given have been reduced to an exposure time of 1 minute, assuming a Schwarzschild exponent of 0.85. The last columns, computed by the writer from data in the preceding columns, the ratios of specific energy, are of especial interest and will be discussed farther on. They are obtained by com-

[2] *Ap. J.*, **76**, 106, 1932.

bining the ratio of areas with the corresponding difference in magnitude, according to the formula

$$\text{R.S.E.} = \left(\frac{d'}{d}\right)^2 \text{antilog } 0.4\delta m \,. \tag{6}$$

Hubble has similar data on limiting magnitudes in the case of the Mount Wilson 10-inch Cook triplet, which show an interesting and significant difference in behavior, compared with the foregoing results from the reflectors, as the partial tabulation of his data shows (Table 4). In this case the threshold images were much smaller in

TABLE 4

LIMITING MAGNITUDES FROM THE 10-INCH COOK TELESCOPE

Diam. of Image		Reduced Mag.
	mm	m
3".6	0.020	12.6
5.0	.028	12.7
12.6	0.070	13.0

linear amount than for the reflectors, which, of course, was to be expected. It is noticed, however, that for the smallest images the efficiency drops 0.4 mag., whereas in the case of the reflectors the efficiency increases up to the smallest images obtained. While this is perhaps not the true explanation, it is suggested that the density necessary for discrimination, for $d = 20\ \mu$, more than outweighs the increase in the concentration of light.

The columns R.S.E. of Table 3 are of especial interest. In the case of the 100-inch telescope it is seen that there is fifty-one times as much energy, per unit of area, falling upon the smallest threshold image as there is upon the largest. In the case of the 60-inch telescope the factor is greater. It will be seen later that the higher photographic density necessary for visibility in the case of the smaller images can account for only a part of the foregoing observed ratio. It has been suggested to the writer by B. Strömgren that a part of the discrepancy may be of atmospheric, optical, or photographic origin, or a combination of all three. A measure of this loss is to be

found in the rate of spreading of focal images, now to be discussed. It is appropriate at this point to call the attention of the reader to the inefficiency of the photographic plate in the utilization of the incident energy. According to the measures of Nutting[3] (discussed by the writer),[4] 57 per cent of the energy incident on the plate is reflected from its front surface, and 35 per cent is transmitted, leaving but 8 per cent for the formation of the latent image. This relation, however, applies to extended images and not to threshold stellar images, in which case there appears another large factor of loss, as will now be shown.

A number of formulae have been proposed connecting the diameter of stellar images with magnitude and exposure time.[5] The Greenwich equation seems to fit modern astronomical observations so well that it will be used as a basis in the present discussion. The formula proposed by the writer[6] is of wider application but is more troublesome in practice, and will, accordingly, not be considered here.

Let r be the radius of a threshold stellar image. Its value will depend on seeing conditions, on the focal length of the telescope, and on its degree of optical perfection. Let the specific illumination over the threshold disk be given by I, and let i be the illumination at any distance x from the edge of the threshold disk. It is shown[7] that an intensity distribution of the form

$$i = Ie^{-k(\sqrt{x+r}-\sqrt{r})} \tag{7}$$

leads to a linear relation between the square root of the diameter of the image and the logarithm of the intensity, or the magnitude, of the form

$$\left.\begin{aligned} \sqrt{d} &= c + \frac{\sqrt{2}}{k}\log_e I\,, \\ \sqrt{d} &= c' - \frac{2}{5}\frac{\sqrt{2}}{k}\frac{1}{\text{mod}}\,m, \end{aligned}\right\} \tag{8}$$

which is the Greenwich equation.

[3] *Trans. Illum. Eng. Soc.*, **10**, 353, 1915.

[4] *The Physics of the Developed Photographic Image*, Mono. 5 (Research Laboratory of the Eastman Kodak Co.), p. 40, 1924.

[5] *Ibid.*, pp. 88–95. [6] *Ibid.*, p. 93. [7] *Ibid.*, p. 95.

Integration of (7) gives the total amount of light surrounding the true or threshold image, from which the fraction P of the total light which is contained in the threshold image follows. Its value is given by

$$\frac{1}{P} = 1 + \frac{4}{k}\left[r^{-1/2} + \frac{3}{k}r^{-1} + \frac{6}{k^2}r^{-3/2} + \frac{6}{k^3}r^{-2}\right]. \tag{9}$$

k is determined from equation (8), using two suitably chosen measured diameters.

It will be of interest to compare the foregoing value of P with the value obtained on the assumption that the light-distribution is given by the well-known Bouguer law

$$i = Ie^{-k_1 x}, \tag{10}$$

which leads to the Scheiner law of growth of image. In this case the value of P becomes

$$\frac{1}{P} = 1 + \frac{2}{k_1^2}\frac{1 + k_1 r}{r^2}, \tag{11}$$

k being given by[8]

$$d = c + \frac{2}{k_1}\frac{1}{\text{mod}}\log_{10} I. \tag{12}$$

Loss of light in focal images.—It has been noted (p. 553) that the loss of light, and therefore the reduction in efficiency of focal images, is due to a combination of photographic, optical, and atmospheric factors, the latter apparently becoming important only for long focal lengths. In support of this I have collected the following data. It will be more convenient to make calculations based on the Scheiner equation (11) since it gives a value of P which is not notably different from the value obtained from the Greenwich formula. The parameter k_1 governing P, in the Scheiner formula, is related to Δ as follows:[9]

$$k_1 = \frac{1.386}{\Delta}p \quad (p = \text{Schwarzschild exponent}). \tag{13}$$

[8] *Ibid.*, p. 94. [9] *Ibid.*, p. 105.

Δ is defined as the uniform increase in the diameter of the focal image, in microns, per doubling of the light-intensity. It is very easily evaluated from any series of observations. A large amount of data on Δ has been collected by the writer from laboratory measures, using a well-corrected lens of short focus.[10] The atmospheric effect is, therefore, zero. In these measures Δ was found to increase notably with increase in wave length, and, in addition, with increase in size of threshold image. A Seed Lantern Slide plate apparently gave as large values of Δ as a plate of larger grain, Seed 23, the values ranging from $\Delta = 8\ \mu$ to $12\ \mu$. The variation with wave length was very large, increasing from $4\ \mu$ at λ 4000 to $17\ \mu$ at λ 6000. Recent laboratory measures by the writer, with Eastman 40 plates, confirm the values 8–12 μ above. Values obtained at the telescope will now be given for comparison. In Ross[11] a number of values of the parameters Δ and d are collected, obtained from data by Parkhurst and Farnsworth at the Yerkes Observatory. Thus, they find for the 40-inch refractor, with Cramer Iso plates, the values $d = 80\ \mu$ and $\Delta = 20\ \mu$. For the 24-inch reflector diaphragmed to 12 inches, with Seed 30 plates, they find $d = 17\ \mu$ and $\Delta = 11\ \mu$. With the same telescope, and Cramer Iso plates, they find $d = 17\ \mu$ and $\Delta = 20\ \mu$, thus confirming the dependence on wave length. These results are substantiated by similar data obtained by them with the 6-inch ultraviolet telescope. For it they find, for Seed 30, the values $d = 14\ \mu$ and $\Delta = 13\ \mu$, the latter increasing to $20\ \mu$ for the Iso plate.

Dr. W. Baade has kindly made exposures of the polar sequence with the Mount Wilson 60-inch telescope (diaphragmed to 40 inches). The seeing was 2. From these I find $\Delta = 35\ \mu$. This large value shows the increasing effect of atmospheric conditions, combined with large focal length. Series of exposures of the same kind with both the 100-inch and the 60-inch telescopes, made under varying seeing conditions, would give valuable data for the calculation of P, the efficiency factor, important in the limiting magnitude problem (p. 566).

II. SENSITOMETRY

By sensitometry is usually meant the process of obtaining the relation between photographic density and the corresponding ex-

[10] *Ibid.*, pp. 99–102. [11] *Ibid.*, p. 100.

posure, $E = It$, for various types of plates, developers, and development conditions. These curves are of importance in the present investigation, as will appear later. The plotted curve of density against log E is called the characteristic, or the Hürter and Driffield (H. and D.) curve.

The so-called tube sensitometer has been used for the present investigation. Since we are interested mainly in the low threshold images, it is important to derive accurate data for the so-called "toe" of the characteristic curve. Accordingly, the intensity steps were made small, in order to have a sufficient number of points for an accurate plotting of the toe. The densities have been measured with the thermoelectric photometer, which is especially well adapted to obtain accurate values of low densities. The accuracy is of the order of 0.002 in density. It is important to note that with this instrument the measured densities are "specular" as opposed to "diffuse." The relation between these is, approximately,

$$D_s = 1.5 D_d . \tag{14}$$

In the following, all densities are specular.

The developer.—It is well known that the characteristic curve exhibits wide variations depending upon the developer and the development conditions. Since it would have been impossible to make extensive tests, which would have been highly desirable, only two developers have been selected for comparison: the widely used Eastman formula D 11 and a pure Metol developer. Their composition is as tabulated.

D 11		Metol	
Metol or Elon	2.7 gm	Metol or Elon	14.0 gm
Hydroquinone	24.0	Sodium sulphite	82.0
Sodium sulphite	187.0	Potassium carbonate	60.0
Potassium carbonate	62.0	Potassium bromide	4.0
Potassium bromide	12.0	Water	80.0 oz
Water	80.0 oz		

D 11 is a moderately "contrasty" developer, exhibiting bromide depression of the toe, building up a high gamma (γ) in the straight-line portion of the characteristic curve and a high density in the highlights. It has proved very useful in spectroscopy and in mensura-

tional problems. The Metol developer is much quicker in action and does not build up the high contrast or density of D 11. The writer has found it useful in photometry, used in connection with the thermoelectric photometer. It is excellent for developing negatives of nebulae containing wide variations in specific brightness.

The results of the comparison of these two developers are shown in Figure 1. The plate is Eastman 40. The dotted curves are for

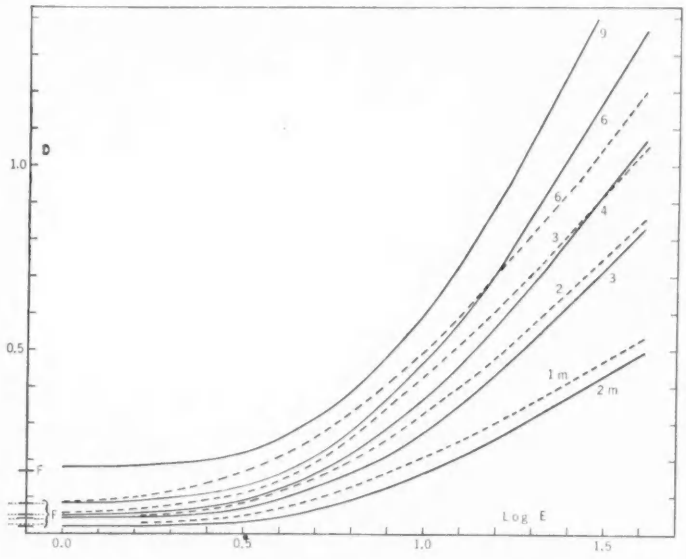

FIG. 1.—Characteristic curves for Eastman 40 plate. Full lines, development in D 11. Dotted lines, development in Metol. The numbers give the time of development in minutes.

Metol; the full curves, for D 11. The numbers give the time of development. The temperature of development was 65°. The corresponding fog densities are shown at the left. Inspection of the curves fully substantiates the statements made above. They show, in addition, that it is useless to push the development time beyond 4 minutes in the case of Metol, and beyond 6 minutes for D 11. The only result is an added density, constant in amount over the entire curve, which is highly undesirable.

Development of a formula relating density to exposure.—Many expressions have been developed[12] relating density to log *E*. None is

[12] *Ibid.*, pp. 47 ff.

of sufficient accuracy for our purpose. Since, in most astronomical problems, specifically in the present one, only the lower portion of the characteristic curve is of importance, the derivation of an accurate formula is simplified. After many trials I have accepted the following functional form:

$$D = c\,(1 - e^{-\kappa I^2})\,. \tag{15}$$

The constants c and κ are determined from two points, one near the threshold and the other at the beginning of the straight-line portion.

TABLE 5

THE DENSITY FORMULA COMPARED WITH OBSERVATIONS

log I	D_f	D_0	log I	D_f	D_0
0.00	0.005	0.004	0.70	0.12	0.13
.10	.008	.005	0.80	.19	.20
.20	.013	.010	0.90	.28	.28
.30	.021	.019	1.00	.39	.39
.40	.033	.032	1.10	.52	.51
.50	.052	.052	1.20	.64	.65
0.60	0.081	0.080	1.30	0.73	0.79

For a test of the formula I have applied it to one of the curves in Figure 1, namely, that of 6 minutes' development in D 11. The formula is, for this case,

$$D = 0.775\,(1 - e^{-0.0070 I^2})\,. \tag{16}$$

Comparison with the observed curve is made in Table 5. The agreement is seen to be very good up to $D = 0.65$, beyond which the formula no longer holds. However, for astronomical purposes, this is quite sufficient. It will be useful to present the characteristic curve in another form, namely, as the density plotted against the exposure (not log E). This has been done in Figure 2. The curve for 6 minutes' development in D 11 (Fig. 1) has been chosen for the transformation. Curves of this type are more useful for astronomical purposes than the customary logarithmic type, for they depict the region of low density much more effectively, and therefore give more accurate data on the speed of emulsions and on contrast in the region of low densities. In addition, they are necessary in evaluating the effect of pre-exposure, as will be shown (p. 574).

It will appear later that it is necessary to have the value of the contrast factor, $\delta D/\delta \log E$, at various density levels, corresponding to the density of the background in long exposures on the sky for limiting magnitudes. Because of its importance, a large number of types of emulsions have been investigated with the object of finding those most suited to the problem of limiting magnitude. The results are collected in Table 6. In preparing this table it was found that

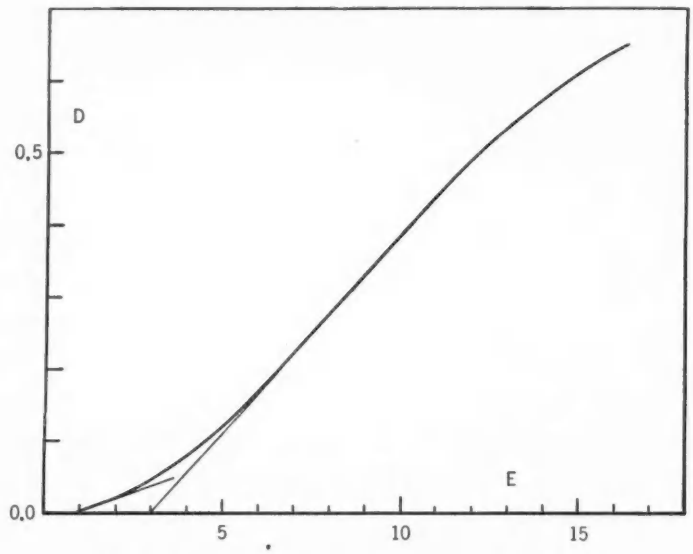

FIG. 2.—Curve of density against exposure (Pl. E 40)

the development time did not affect the values, except for large values of D and for underdevelopment and overdevelopment. It is noted that D 11 gives slightly higher values than Metol, and that, for the blue-sensitive emulsions, the values of contrast are in inverse relation to their speed. The highest values are for Eastman 1 G, and for Wratten and Wainright Panchromatic plates, both used with yellow filter.

There may be some question as to the applicability of these determinations of the contrast factor, γ, to the astronomical problem, because of the very great differences in the intensities involved, and because of color differences. With regard to the color differences, there is undoubtedly an effect, but it should be small, certainly not

more than 10 per cent. The faint stars concerned are reddened by space absorption, and thus approximate in color to unscreened laboratory sources of light. From considerations involving the penetration of light in an emulsion, combined with reciprocity failure, one might expect a dependence of γ on intensity. There are very decisive data to the contrary. Jones and Huse[13] found no variation whatever over a range in light-intensity of one to a million.

TABLE 6

VALUES OF γ AT VARIOUS DENSITY LEVELS

Dens.*	East. Process	E 33	E 40		Imp. Ecl.		East. 1 G	W.W. Pan.	Agfa Film
	D 11	D 11	D 11	Metol	D 11	Metol	D 11	D 11	D 11
0.02	0.11	0.09	0.10	0.10	0.09	0.06	0.11†	0.10†	0.10‡
0.04	0.20	0.18	0.20	0.19	0.17	0.12	0.23	0.20	0.20
0.06	0.28	0.28	0.28	0.27	0.24	0.18	0.33	0.31	0.30
0.08	0.37	0.36	0.35	0.34	0.30	0.24	0.41	0.41	0.39
0.10	0.46	0.43	0.42	0.41	0.36	0.30	0.50	0.52	0.46
0.15	0.67	0.58	0.54	0.53	0.48	0.42	0.74	0.75	0.62
0.20	0.80	0.71	0.64	0.62	0.58	0.52	0.94	0.95	0.78
0.25	0.93	0.82	0.75	0.69	0.66	0.58	1.10	1.11	0.92
0.30	1.04	0.90	0.85	0.76	0.73	0.64	1.21	1.27	1.04
0.35	1.17	0.97	0.93	0.82	0.80	0.69	1.31	1.41	1.14
0.40	1.29	1.03	0.99	0.88	0.86	0.73	1.41	1.53	1.24
0.45	1.39	1.10	1.05	0.93	0.91	0.79	1.50	1.66	1.33
0.50	1.50	1.16	1.11	0.99	0.96	0.83	1.57	1.79	1.40
0.60	1.72	1.29	1.24	1.09	1.06	0.95	1.70	2.00	1.52
0.80	2.12	1.54	1.52	1.27	1.24	1.16	1.92	2.24	1.63
1.00	2.50	1.77	1.59	.....	1.42	.....	2.12	2.42	1.69
1.20	.....	1.99	1.59	.....	.....	.....	2.23	2.54	1.71
1.40	.....	2.15	.....	.....	.....	.....	2.53	2.63	.....
1.60	.....	.....	.....	.....	.....	.....	2.73	.....	.....

* The fog has been subtracted from the density.
† With yellow filter. ‡ With red filter.

III. LABORATORY RESULTS FROM THRESHOLD IMAGES

It will now be necessary to obtain data on:

a) The density level of the background exposure which will allow the faintest limiting magnitude to be reached. It is well known that the rate of appearance of the fainter stars on a photographic exposure falls off with increasing sky density, finally becoming zero

[13] *J. Opt. Soc. Am.*, **7**, 100, 1923.

or even negative when a certain density has been reached. This density value is an important parameter in any evaluation of limiting magnitude, for it is the argument of Table 6, giving the contrast factor, γ, which enters into the equation for limiting magnitude.

b) The equation for limiting magnitude will be found to contain, in addition to γ, the difference in density between the threshold image and its background δD. Accurate data on this important quantity are not available at present. In the limiting case of a grainless emulsion, it can be put equal to 0.01. In the case of actual emulsions, its value has been merely guessed, or estimated from the appearance of the clustered grains forming the threshold image, or specifically from its grayness. Theoretically, a count of the grains would lead to an approximate value of the density, but this would be difficult because of the distribution in depth of the grains in the emulsion. It is necessary to devise some method of actual measurement. For this purpose the writer has had made a template of metal, containing a series of round holes of graduated sizes. It is shown, in actual size, in Figure 3. It contains, in addition, a slit, for data on spectral lines. It is illuminated from behind with light from a series of diffusing opal glasses, carefully adjusted for uniform illumination over the area covered by the holes. Photographs are then made, with a well-corrected lens of 5 inches focal length, the distance of the template being such as to produce artificial star images on the plate approximating in diameter the threshold images obtained in telescopes of moderately long focal length. Exposures were made at two distances, the reduction factors for which were 15.86 and 20.93. The corresponding diameters of the images, computed from the measured diameters of the template holes and the foregoing reduction factors, are contained in Table 7.

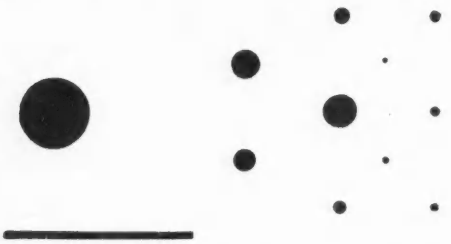

FIG. 3.—Template giving artificial star images.

Since the holes are equally illuminated, it can be assumed that the specific intensity of the light falling on the photographic plate

is the same for all the images. With regard to the effective intensity within the emulsion, this, however, is not true, for there is a loss depending on the size of the image and on k (p. 555). The Eberhard effect must necessarily be neglected; because of the low densities involved, it must be small. The problem is now to obtain the true densities of the threshold images. It is possible to measure the densities of the three largest images, a, b, and c, with the thermoelectric photometer. In order to obtain the densities of the smaller

TABLE 7

DIAMETERS OF ARTIFICIAL STAR IMAGES

HOLE	DISTANCE		HOLE	DISTANCE	
	A	*B*		*A*	*B*
	mm	mm		mm	mm
a	0.602	0.456	*h*	0.091	0.069
b	.287	.217	*i*	0.081	0.062
c	.244	.185	*j*	0.066	0.050
d	.190	.144	*k*	0.054	0.041
e	.145	.110	Slit	0.048	0.036
f	.121	.092	Slit length	1.600	1.200
g	0.103	0.078			

images it is necessary to compute the loss of light from equation (9), and to apply Table 5 to transform it into density.

The laboratory investigation was limited to one kind of plate, one developer, and one development time, although it would have been highly desirable to obtain results for other plates. The plate chosen was Eastman 40, for it represents the best compromise; the developer was D 11; the development time was 6 minutes at 65°. A number of exposures were made on each plate, the time being varied in order to obtain images from below threshold to overexposure. The background exposure was obtained by removing the template. Measurement of each plate consisted in (*a*) judging the threshold images, under low magnification; (*b*) measuring the diameters; and (*c*) measuring, with the photometer, the density of fog over clear glass; the density of the background exposure over fog D_{BG}, and the density of images a, b, and c with respect to the background density D_i. A large number of plates were thus exposed

and measured. The range in background density is from 0.00 to 0.93. The fog amounted to 0.08, which has been subtracted in all cases. The results have been plotted, first against density and then against size of image. From this system of curves a double-entry table has been constructed (Table 8).

In Table 8, d is the diameter of the threshold image and D_{BG} the specular density of the pre-exposure with respect to the development

TABLE 8

THRESHOLD DENSITIES, D_i

d	D_{BG}						
	0.00	0.10	0.20	0.30	0.40	0.50	0.90
mm							
0.040	0.51	0.38	0.32	0.28	0.25	0.24	0.23
.050	.35	.24	.19	.18	.17	.17	.17
.060	.27	.17	.13	.12	.12	.12	.12
.070	.20	.13	.09	.08	.08	.08	.08
.080	.14	.10	.07	.06	.06	.06	.06
.090	.10	.08	.06	.05	.05	.05	.05
.100	.08	.06	.05	.04	.04	.04	.04
.120	.05	.05	.05	.04	.04	.04	.04
.150	.04	.04	.04	.04	.04	.04	.04
.200	.03	.03	.03	.03	.03	.03	.03
0.400	0.01	0.01	0.01	0.01	0.01	0.01	0.01

fog. The threshold densities of Table 8 must now be corrected for loss of light. The amount of light in the threshold image can be computed from equation (9), the parameter k being obtained from measures of diameter, in accordance with equation (8). The results are given in Table 9. The values of k are obtained from a smooth curve. The column P' contains the ratio of P to the value for $d=0.400$ mm.

Making use of Table 9, giving the percentage of light in threshold images, and the characteristic curve for Eastman 40 (development 6 minutes in D 11), Figure 1, Table 10, containing the corrected density for the threshold template images, can be formed. It is to be noted that the column P', Table 9, must be used, since the measured densities of Table 8 are for the largest template image.

It is surprising to note from the table that the threshold difference

in density between image and background decreases with increase in background density (see p. 569).

TABLE 9

PERCENTAGE LIGHT IN TEMPLATE THRESHOLD IMAGES

d	k	P	P'	d	k	P	P'
mm				mm			
0.040	1.26	0.446	0.52	0.100	1.42	0.649	0.76
.050	1.29	.498	.58	.120	1.47	.685	0.80
.060	1.31	.538	.63	.150	1.55	.730	0.85
.070	1.34	.571	.67	.200	1.69	.781	0.91
.080	1.36	.599	.70	0.400	1.87	0.855	1.00
0.090	1.39	0.625	0.73				

TABLE 10

DENSITIES D_i OF THRESHOLD TEMPLATE IMAGES

(Corrected for light-loss)

d	BACKGROUND DENSITY						
	0.00	0.10	0.20	0.30	0.40	0.50	0.90
mm							
0.040	0.24	0.21	0.19	0.15	0.14	0.13	0.13
.050	.15	.14	.11	.11	.10	.10	.10
.060	.12	.11	.08	.08	.08	.08	.08
.070	.10	.09	.06	.05	.05	.05	.05
.080	.07	.07	.05	.04	.04	.04	.04
.090	.05	.05	.05	.04	.04	.04	.04
.100	.04	.04	.04	.03	.03	.03	.03
.120	.04	.04	.04	.03	.03	.03	.03
.150	.03	.03	.03	.03	.03	.03	.03
.200	.02	.02	.02	.02	.02	.02	.02
0.400	0.01	0.01	0.01	0.01	0.01	0.01	0.01

Formula for limiting magnitude.—Let the specific intensity of the sky background be B_0, and let the brightness of a star at threshold be $r \cdot B_0$. The brightness of the image will be

$$B_i = (1 + r)B_0 ,$$

and

$$\delta \log B_i = \log (1 + r) . \qquad (17)$$

The relation between r and the magnitude difference is

$$\delta m' = -2.5 \log r . \tag{18}$$

Passing to the photographic plate, we have

$$\left.\begin{aligned} &\delta D = \frac{\partial D}{\partial \log E}\,\delta \log E; \qquad (E = It) \\ \text{or} \quad &\delta D = \gamma\,\delta \log E . \end{aligned}\right\} \tag{19}$$

γ is the contrast factor of the emulsion, and must not be confused with maximum contrast, to which the term usually applies. Its value is given in Table 6. Neglecting the time factor t, and putting $\delta D = D_i$, equations (17) and (19) give

$$\log (1 + r) = \frac{D_i}{\gamma} . \tag{20}$$

Equation (18) gives $\delta m'$. The limiting magnitude is then

$$m_l = \text{Table } 2 + \delta m' . \tag{21}$$

In the special case of δD small compared with γ, we have

$$m_l = \text{Table } 2 - 2.5 \log \left[\frac{D_i}{\text{mod } \gamma}\right] . \tag{22}$$

Computation of dm′.—It is now possible to form the quotient D_i/γ, from Tables 10 and 6. It is important to note that in obtaining γ from Table 6 the argument of entry is D(background) $+ \frac{1}{2}D_i$. The values of dm', or the corrections which must be applied to the values of Table 2, are computed from equations (20) and (18). The result is contained in Table 11.

It is necessary to apply a second correction, dm'', depending on the loss of light in the threshold image, which is a function of the particular telescope and observing conditions as well as of the kind of plate, its color sensitivity, and filter. Its value is, obviously,

$$dm'' = 2.5 \log P . \tag{23}$$

The final limiting magnitude is

$$m_l = \text{Table } 2 + dm' + dm'' . \qquad (24)$$

Exposure times.—It is important to correlate background densities with exposure times. To this end a very transparent night in September, 1937, was chosen, and an exposure made to the sky with the Yerkes 24-inch reflector, on an Eastman 40 plate, the exposure time being 32 minutes. The density of the sky background with respect to the density of the development fog was found to

TABLE 11

VALUES OF dm'

d	Background Density					
	0.10	0.20	0.30	0.40	0.50	0.90
mm	m	m	m	m	m	m
0.040	−0.1	+0.4	+0.9	+1.1	+1.3	+1.7
.050	+0.2	1.0	1.3	1.5	1.6	2.0
.060	0.5	1.4	1.6	1.8	1.9	2.3
.070	0.8	1.7	2.1	2.3	2.4	2.7
.080	1.1	1.8	2.3	2.5	2.7	2.9
.090	1.4	1.9	2.5	2.6	2.8	3.1
.100	1.6	2.0	2.6	2.7	2.9	3.3
.120	1.7	2.2	2.7	2.8	3.0	3.5
.150	1.9	2.4	2.8	2.9	3.1	3.5
.200	2.3	2.8	3.1	3.3	3.5	3.8
0.400	+3.1	+3.5	+3.8	+4.0	+4.2	+4.4

be 0.060. Applying the characteristic curve (Fig. 1) and taking account of the reciprocity failure, it becomes a simple matter to compute the exposure time for any specified background density and any speed ratio. The results are given in Table 12.

Limiting magnitudes for long exposures.—Long exposures correspond to high background densities, reaching the highest values in Table 12, namely, 0.90, and higher. It is at once apparent from an inspection of Table 11 that a higher efficiency is predicted for the long exposures than is actually obtained in practice. This can be traced to the diminution in the densities of the threshold template images, D_i, with increasing background density (Tables 8 and 10). This result was unexpected, but was supported by so much material

that it could not be ignored. A qualitative physical explanation is as follows: The visibility of a dispersed aggregation of silver grains is improved, up to a certain point, by an added uniformly dispersed

TABLE 12

EXPOSURE TIMES, EASTMAN 40 PLATE

DENS. *BG*	SPEED RATIO						
	1.5	2.0	3.0	3.3	4.0	5.0	6.0
	h	h	h	h	h	h	h
0.10	0.1	0.2	0.5	0.6	0.8	1.3	1.8
.20	.2	0.3	0.7	0.8	1.2	1.9	2.7
.30	.2	0.4	0.9	1.0	1.5	2.4	3.6
.40	.3	0.5	1.1	1.3	1.9	3.0	4.3
.50	.3	0.6	1.3	1.6	2.4	3.7	5.3
0.90	0.6	1.1	2.5	3.0	4.4	6.8	9.9

TABLE 13

dm'

(Assuming D_i the same for all D_{BG})

d	D_{BG}						Δ
	0.10	0.20	0.30	0.40	0.50	0.90	
mm	m	m	m	m	m	m	m
0.040	−0.1	+0.3	+0.5	+0.6	+0.8	+1.1	+1.2
.050	+0.3	0.7	1.0	1.1	1.3	1.6	1.3
.060	0.6	1.0	1.3	1.4	1.5	1.9	1.3
.070	0.8	1.2	1.5	1.6	1.8	2.1	1.3
.080	1.1	1.5	1.8	1.9	2.1	2.4	1.3
.090	1.4	1.9	2.1	2.3	2.4	2.8	1.4
.100	1.7	2.1	2.4	2.6	2.7	3.0	1.3
.120	1.8	2.2	2.5	2.7	2.8	3.2	1.4
.150	2.0	2.4	2.7	2.9	3.0	3.4	1.4
.200	2.5	2.9	3.1	3.3	3.4	3.8	1.3
0.400	+3.2	+3.6	+3.9	+4.0	+4.2	+4.6	+1.4

grain system, causing clustering effects and leading to visibility. From Table 11 it is seen that the gain in magnitude, from the background density 0.10–0.90, averages 1.8 mag. This corresponds to a

fivefold increase in exposure time (Table 12). Accurate data are not available, but I would estimate that the gain is actually of the order of 1.2 mag., noting from Table 12 that the corresponding exposure times are, for F/5, 1.3 and 6.8 hours, respectively. It might possibly be found that a variation of the third term in the limiting magnitude, dm'', may take up a part of the difference. Lacking data on this point, it will be of interest to make a recomputation of Table 11, giving dm', on the very reasonable assumption that the density D_i of the threshold image with respect to its background does not differ from the values for the background density of 0.10 of Table 10. The results of the recomputation are contained in Table 13.

Limiting magnitude, Yerkes 24-inch reflector.—For this telescope I have determined $k = 0.86$, from an exposure to the polar sequence. Because of the uncertainty in the value of the threshold diameter, d, the calculation for limiting magnitude will be made for three values. Results for $D_{BG} = 0.10$ are tabulated.

d	0.040 mm	0.035 mm	0.030 mm
	m	m	m
Table 2	19.4	19.8	20.1
Table 13 (dm')	− 0.1	(− 0.3)*	(− 0.5)*
Eq. (23) (dm'')	− 1.3	− 1.4	− 1.5
Sum	18.0	18.1	18.1

* Extrapolated.

From Table 12 the corresponding exposure time for an Eastman 40 plate is 0.8 hour. With an exposure pushed to the limit, for which the background density can be taken equal to 0.90, the gain will be 1.2 mag. (Table 13). The corresponding exposure time is 4.4 hours.

Limiting magnitude, Lick 36-inch reflector (Crossley).—From plates of the polar sequence furnished me by Dr. N. U. Mayall, I find $k = 0.96$. The smallest images obtained with this telescope under the best conditions, with short exposures, are of the order of 0.030 mm in diameter. The computation for limiting magnitude should, how-

ever, be made for the larger values applicable to long exposures. The results for $D_{BG} = 0.10$ are shown in the accompanying table.

d	0.060 mm	0.050 mm	0.040 mm
	m	m	m
Table 2	20.3	20.7	21.2
Table 13 (dm')	+ 0.6	+ 0.3	− 0.1
Eq. (23) (dm'')	− 1.0	− 1.1	− 1.2
Sum	19.9	19.9	19.9

The corresponding exposure time is 1.7 hours (Table 13).[14] With regard to the actual performance of this telescope, Mayall writes substantially as follows: "With Imperial Eclipse Plates, the average limiting magnitude is 19.8 for 60-minute exposures with a threshold diameter of 2″.0–2″.5 (50–60 μ); the best plate shows 20.2, with a threshold diameter of 1″.5 (40 μ)."

Limiting magnitude, Mount Wilson 60-inch reflector.—From plates of the polar sequence by W. Baade (seeing 2), I find $k = 0.79$. From a long-exposure plate by F. H. Seares (seeing 5), I find $k = 0.95$, showing a distinct gain for the improvement in seeing. Using the latter value, the results of the computation are as tabulated. The

d	0.060 mm	0.050 mm	0.040 mm
	m	m	m
Table 2	21.1	21.5	22.0
Table 13 (dm')	+ 0.5	+ 0.2	− 0.1
Eq. (23) (dm'')	− 1.0	− 1.1	− 1.2
Sum	20.6	20.6	20.7

corresponding exposure time, with an Eastman 40 plate, is 1.3 hours. Strictly, it is not correct to use the same value of k in the computation of dm'' for different values of d, for both k and d depend on seeing conditions. Thus, for $d = 0.060$ mm, the seeing would be poor, so that the value $k = 0.79$ should have been used, giving $dm'' = -1.2$ and a final magnitude of 20.4. The range in limiting magnitude from good to poor seeing then becomes 0.3 mag., which is in good agreement with the values in Table 3.

[14] Not corrected for prime focus.

Analysis of Hubble's data, for light-efficiency.—It is now possible to carry the computations of Table 3 a step farther, since values of the threshold density for all values of the diameter of the threshold image are now available (Table 10). The results are to be found in Table 14. The third column gives the density correction, computed

TABLE 14

EFFICIENCY OF FOCAL IMAGES, FROM HUBBLE'S DATA

d	Hubble m	$\Delta m'$	$\Delta m''$	m_c	Δm	L.E. = P
	Mount Wilson 100-Inch					
mm	m	m	m	m	m	
0.054	17.03	1.25	0.00	18.28	2.21	0.13
0.069	17.03	1.10	0.51	18.64	1.85	0.18
0.075	17.15	0.98	0.71	18.84	1.65	0.22
0.081	16.70	0.92	0.88	18.50	1.99	0.16
0.087	16.92	0.75	1.03	18.70	1.79	0.19
0.100	16.75	0.62	1.33	18.70	1.79	0.19
0.106	16.83	0.62	1.46	18.91	1.58	0.23
0.137	16.19	0.50	2.02	18.71	1.78	0.19
0.194	16.10	0.30	2.78	19.18	1.31	0.30
0.413	15.75	0.00	4.41	20.16	0.33	0.74
0.906	14.37	0.00	6.12	20.49	0.00	1.00
	Mount Wilson 60-Inch					
0.040	16.60	1.61	0.00	18.21	2.43	0.11
0.052	16.60	1.32	0.57	18.49	2.15	0.14
0.059	16.25	1.20	0.85	18.30	2.34	0.12
0.066	16.40	1.15	1.09	18.64	2.00	0.16
0.074	16.50	1.05	1.33	18.88	1.76	0.20
0.092	16.20	0.75	1.81	18.76	1.88	0.18
0.099	16.18	0.62	1.97	18.77	1.87	0.18
0.370	14.80	0.00	4.83	19.63	1.01	0.40
0.660	14.00	0.00	6.08	20.08	0.56	0.60
1.290	13.10	0.00	7.54	20.64	0.00	1.00

from Table 8 and from the characteristic curve, Figure 1. The fourth column gives the geometrical correction for size of image; the fifth gives the corrected magnitude; and the sixth, the deficiency in limiting magnitude for each size of image as compared with the value in the last row. In the seventh column this has been converted into light-efficiency. It is important to evaluate the effect of possible

errors in the data upon the values in the sixth and seventh columns. For the 100-inch, for $d = 0.054$, assume that there is an error in the measurement of d and that it is larger by 0.010 mm. The correction to Δm becomes -0.35 mag., an unimportant amount. Assume, further, that the density D_i obtained from Table 10 is too small, that it is 0.28 for the smaller images. Carrying through the computation, combining with the assumed correction to the diameter, we find $\Delta m = 1.35$ and $P = 0.35$, in good agreement with the value resulting from the known value of k for the 60-inch telescope. Values of k for the 100-inch telescope are not available.

The confusion disk.—The diameter of the diffraction disk for various telescopes has already been given (p. 549). A small value is of the greatest importance in the measurement of close double stars, and in the delineation of planetary detail. Unfortunately, when photography is employed, a number of factors increase the "diffraction" diameter by a factor of the order of 10–20, giving an optical disk which has been called the "confusion disk." The various factors determining the size of the confusion disk will now be considered.

a) Spherical and chromatic aberrations.—In the case of lenses, both spherical and chromatic aberration are factors, while for mirrors we have only spherical aberration, if atmospheric dispersion is excepted. It will be of interest to give the results of some computations on the size of the disk produced by spherical aberration, in the case of the Yerkes 40-inch refractor, and the 24-inch reflector, data for the computation in each of these cases being available. Philip Fox[14a] found in the case of the 40-inch refractor that the edge zone focuses 8 mm beyond the focus for the center and 3 mm beyond the focus for the zone at a radius of 330 mm, the zone at two-thirds of the aperture. This difference of 3 mm is the quantity which enters into the formula for the diameter of the confusion disk, unless very abnormal zonal errors are present. Calling it Z, it is easy to show that the resulting diameter of the confusion disk is

$$G = \frac{3}{8}\frac{D}{F}Z, \tag{25}$$

[14a] *Ap. J.* **27**, 241, 1908.

in which D and F are the diameter and the focal length, respectively, of the lens. Inserting numerical values and $Z = 3.0$, we have

$$G = 0.052 \text{ mm} .$$

The effect of chromatic error is difficult to evaluate; it should, however, be small. The smallest value which has ever been obtained for the confusion disk in the case of this telescope is of the order of 0.075 mm, which agrees well with the value calculated above, allowance being made for atmospheric effects.[15]

Alice Farnsworth[16] has made measures of the zonal errors of the Yerkes 24-inch reflector, from which I have calculated $G = 0.030$ mm. This is of the order of the smallest threshold images obtained with this mirror.

It is of some interest to apply the formula for the diameter of the confusion disk to the 200-inch mirror now under construction. Assuming a normal undercorrection or overcorrection for the zones, formula (25) can be applied, giving $G = 0.114Z$, from which it appears that a value of Z as large as 0.3 mm can perhaps be tolerated. In angular value this is a disk $0''.42$ in diameter.

Atmospheric effects will now be considered. The action is of two kinds, namely, an expansion into a disk of diffused light, which may be as large as $10''$; and unsteadiness, or vibratory motion of the image, the frequency of which is too great to be followed in actual guiding. It has been taken for granted that under the best seeing conditions the diameter of the confusion disk, due to atmospheric irregularities, is of the order of $1''.0$. It is of interest to note that this is the value of the total amplitude of atmospheric fluctuations of com-

[15] At first sight it seems difficult to reconcile the size of the optical circle of confusion with the actual resolving power, visually, of refractors, which in general equals their theoretical value. Thus, for the 40-inch telescope the diameter of the circle of confusion is five times the actual visual resolving power. The explanation is to be found in the fact that in visual work—e.g., on double stars—the observer focuses on the greatest concentration of light, which, in the case of the 40-inch telescope, is that from the outer zone, other zones being therefore out of focus and unconsciously disregarded, as are color effects. Consequently, provided the lens is free from astigmatism and glass defects, the theoretical resolving power will be reached—in fact, increased, as Rayleigh has shown.

[16] *Pub. Yerkes Obs.*, **4**, Part V, p. 18, 1926.

paratively long period, the period being of the order of one minute. These fluctuations were discovered by Nusl and Fric, and were investigated by Schlesinger,[17] who found them present even under the favorable conditions at Mount Wilson. The existence of a fluctuation of this type calls for the most precise and attentive guiding, if best results are to be obtained.

There remains the question of the relation between the diameter of the threshold photographic image and the optical circle of confusion. Obviously, the latter, in telescopic exposures, cannot be defined with any accuracy. The best that can be done is to obtain data in the laboratory, using short-focus lenses of the best definition. Results obtained by the writer[18] are contradictory, while recent results from the measurement of the template images (p. 563) show that the photographic threshold image is, on the average, 0.010 mm less than the optical image. This is to be expected, because of scattering of light at the true edge of an optically produced image. In all conclusions, therefore, based on measured values of threshold images, it is well to keep in mind an uncertainty of 10 μ in its diameter, compared with the corresponding optical circle of confusion.

IV. PRE-EXPOSURE

Effects of pre-exposure, predictable from the characteristic curve.— In order to evaluate the effect of pre-exposure it is necessary to replot the characteristic curve, with $E(=It)$ as abscissa, which has been done in Figure 2. For greater accuracy it will be useful to tabulate D in terms of I for $I < 11.0$, making use of formula (13). This has been done in Table 15.

Table 15 shows that with a pre-exposure producing a density of 0.28, a given small exposure produces 3.5 times the density increment that the same exposure would produce at the pre-exposure level of 0.005. This factor, 3.5, would apply to cases where the discrimination factor is small, as in extended surfaces. In the case of star images, however, it is necessary to take into consideration the fact that much greater differences of density are concerned. For small images it has been shown that D_i is in the neighborhood of 0.20. With this

[17] *Pub. Allegheny Obs.*, **3**, 8, 1916.

[18] *Physics of the Developed Photographic Image*, pp. 99–101.

in mind, the accompanying tabulation can be made from table 15. From this it is seen that the maximum efficiency is at the background

TABLE 15

PHOTOGRAPHIC DENSITY AGAINST EXPOSURE

I	D	Diff.	I	P_3	Diff.
1.0	0.005	0.016	9.0	0.335	0.025
2.0	.021	.026	10.0	.390	.040
3.0	.047	.035	11.0*	.430	.050
4.0	.082	.042	12.0*	.480	.040
5.0	.124	.049	13.0*	.520	.040
6.0	.173	.052	14.0*	.560	0.040
7.0	.225	.055	15.0*	0.600	.....
8.0	0.280	0.055			

* D from curve, Fig. 1.

density or pre-exposure level of 0.225, the efficiency falling off on either side. With respect to a very small or no pre-exposure, the efficiency at the 0.225 level is 1.5. It is instructive to compare this efficiency with that in the first case considered, namely, where very small density differences were detectable, of the order of 0.016,

I	ΔI	ΔD	D_{BG}
7.0— 1.0	6.0	0.220	0.005
11.0— 7.0	4.0	.220	.225
15.0—10.0	5.0	0.225	0.395

which applies to large surfaces. It is seen that the efficiency has dropped to less than one-half.

Pre-exposure, with stellar images.—It has just been seen that in the case of extended images pre-exposure is of value in increasing relative contrasts and, therefore, visibility. It is of importance to investigate whether a similar advantage accrues in the case of stellar images. For this case it is necessary to make a study of the cross-section of stellar images. This has been done for six cases, involving three background densities, 0.00, 0.25, and 0.50, and two values of k, namely, 1.26 and 0.79, corresponding respectively to the laboratory template images and to stellar images obtained with the Mount

Wilson 60-inch reflector for poor seeing. The results are plotted in Figure 4. The stellar image considered is one having a diameter $d = 0.040$ mm, and a density, with clear background, equal to 0.25, which corresponds very closely to a threshold image. On examining the sections, if conclusions were to be drawn solely from the differences of density between image and background (col. 2, Table 16), an improvement, with a maximum near $D = 0.25$, similar to that

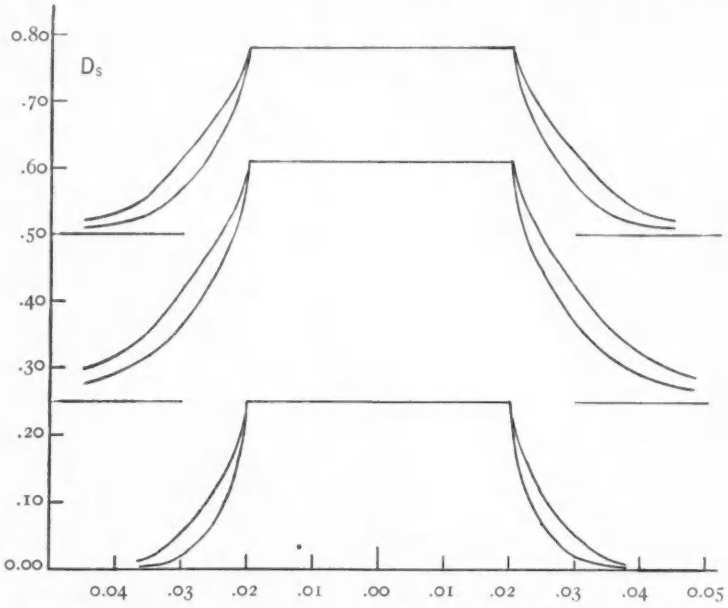

FIG. 4.—Cross-sections of stellar images, with and without pre-exposure. Inner curves, for $K = 1.26$; outer, for $K = 0.79$.

found for extended images, is noted. However, in the matter of the visibility of faint threshold stellar images a different criterion must be applied. This criterion is the rate of fall in density. This is easily obtained from the curves. A tabulation has been made (Table 16) for the fall in density, for $x = 5\ \mu$ and $x = 10\ \mu$, x being the distance from the edge of the threshold image. This criterion shows clearly that the greatest efficiency is obtained with no pre-exposure, with only very slight falling-off for pre-exposures giving a density up to 0.25, after which the falling-off is more rapid. It will be seen

that these conclusions agree with results actually found at the telescope, but are not in agreement with results found from the template images. These latter results correspond to the values of ΔD in Table 16, which apply directly to extended images. The images of the holes in the template are actually disk images, of a different character than those occurring at the telescope. It is therefore reasonable to conclude that the same discrimination factor applies to these images as applies to more extended images.

Observational data on pre-exposure.—A careful study was made of the plates which were exposed to the template (p. 562) to determine

TABLE 16

FALL IN DENSITY: TABULATION FROM FIGURE 4

DENS. *BG*	ΔD	$x = 5\,\mu$		$x = 10\,\mu$	
		$k = 1.26$	$k = 0.79$	$k = 1.26$	$k = 0.79$
0.00	0.25	0.18	0.14	0.23	0.19
.25	.36	.17	.12	.24	.18
0.50	0.28	0.14	0.10	0.21	0.16

the effect of pre-exposure on the visibility of threshold images. The advantage of the pre-exposure was unmistakable for all background densities from 0.10 to 0.50, the optimum effect being at density of 0.20. For images of all sizes, with pre-exposure, the exposure time could be cut in half, for threshold visibility. In the case of the artificial spectrum line (Fig. 3) the factor was increased to 3. In order to see if the advantages of pre-exposure were realized in stellar exposures, tests were made with three instruments, as follows: (*a*) Yerkes 24-inch reflector, observations by the writer—plates: Eastman 40, Eastman Ortho Press, and Imperial Eclipse; (*b*) Yerkes 40-inch refractor, observations by E. G. Ebbighausen—plates: W. and W. Panchromatic and Eastman 1G; (*c*) Mount Wilson 60-inch reflector, observations by Dr. W. Baade—plate: Eastman 40.

a) A large number of plates were exposed, with varying density of background. The mean results are given in Table 17 (exposure time, 2 minutes).

The results are unmistakably opposed to the idea of any advantage of pre-exposure.

b) Exposures were made by E. G. Ebbighausen with the Yerkes 40-inch refractor on two nights, using Eastman 1G, Wratten and Wainright Panchromatic plates, with and without pre-exposures. The threshold images were large, of the order of 0.120 mm. For this reason it was thought that pre-exposures would show a gain, corresponding in some measure to the gain for the disk images of the template. This, however, was not realized: on the average, a distinct loss accompanied the pre-exposed plates. Since the plates were

TABLE 17

LIMITING MAGNITUDE, YERKES 24-INCH REFLECTOR

Background Dens.	Limiting Mag.	No. Plates
	m	
0.00	15.1*	9
.13	15.1	5
.28	15.0	4
.47	14.7	6
0.77	14.4	4

* Maximum limiting magnitude, 16.1; plate, Imperial Eclipse.

exposed to the polar sequence, it was possible to compute k and P. These were, respectively, $k = 0.43$, $P = 0.24$, and $dm'' = 1.5$ mag.

c) Four plates were exposed by W. Baade with the Mount Wilson 60-inch telescope, two of which had pre-exposures of density 0.30. The emulsion was Eastman 40. On the average, the pre-exposed plates were found to give slightly inferior results. The results from all three telescopes are therefore in agreement in showing little or no effect of pre-exposure on limiting magnitude, there being neither gain nor loss for small densities of pre-exposures, but a distinct loss for increasing densities, as can be seen from Table 17.

Brightness of the night sky.—The value of the brightness of the night sky which has been chosen in this investigation, namely, 22 mag. per square second, on the photographic scale, is the value found both by Stebbins and by Elvey from independent investigations, at

Mount Wilson and at Mount Locke, respectively, with the photoelectric photometer. It is subject to considerable variation, owing to changes in the permanent or generally invisible auroral light, first studied by V. M. Slipher. It varies also with the location in the sky with respect to the zodiacal light, which has been found by Elvey to have a brightness, at 90° from the sun on the ecliptic, equal to the foregoing value of the general sky brightness. A recent photographic determination by Jessie Rudnick,[19] at Mount Locke, confirms the foregoing value. I have computed, from the curves given by her, a value of 21.8 mag. for the photographic region, and a value of 21.0 mag. for the red, giving a color index of 0.8 mag. The green auroral line has been excluded in the determination of both of these values. Her investigation was largely concerned with determining the variation with zenith distance. This was found to be small up to a zenith distance of 40°, beyond which the increase in sky brightness was considerable, especially in the red. The value of the sky brightness for the red, 21.0 mag., is subject to very large variations, much greater than for the blue, because of variations from night to night of the invisible aurora. Because of the increasing use of the modern very rapid red sensitive plates in long exposures, as in the recent very notable work by Baade at Mount Wilson, the brightness of the sky in red radiation, and its variations, becomes a matter of the greatest importance.

YERKES OBSERVATORY
July 30, 1938

[19] *Ap. J.*, **87**, 584, 1938.

THE THEORY OF THE COLORS OF REFLECTION NEBULAE

L. G. HENYEY AND JESSE L. GREENSTEIN[1]

ABSTRACT

A theory based on a rigorous treatment of the transfer of radiation through a nebula is needed to interpret observations of the colors of reflection nebulae. Nebulae are, in general, bluer than the illuminating stars because of the greater scattering coefficient of interstellar material in blue light. The nature of the relative color of nebula and star is studied for several different geometrical configurations by the use of idealized models. If the star is in front of the nebula, the color of the nebula will approach that of the star with increasing total opacity. If the nebula is in front of the star, it will always be bluer than the star. The validity of certain approximations used in this discussion is investigated. Possible variations of the scattering efficiency, or albedo, with wave length can contribute strongly to the colors of the nebulae.

The properties of small particles, relevant to the problems of nebular illumination, are derived on the basis of the Mie theory. The observed dependence of the extinction coefficient upon wave length may be explained by the presence of metallic particles, or of an appropriately chosen mixture of dielectric particles of various sizes. The albedo of metallic particles is small and varies with wave length, providing a possible test for the existence of metallic substances in space. The phase function for small particles of various substances is also studied.

INTRODUCTION

The properties of interstellar matter can be studied by means of either transmitted or scattered radiation. The former has been used extensively to show that the extinction coefficient of interstellar matter varies nearly as λ^{-1}. The study of the properties of the scattered radiation is considerably less simple, primarily because the geometrical configuration of the star and the scattering material plays a fundamental role in the size, brightness, and color of the observed nebula. In this investigation we limit our attention to the color effects that may be observed in bright diffuse nebulae having continuous spectra, and we intend to show how these effects depend upon the geometrical and physical properties of the nebulae.

It is easy to see why a theoretical discussion of the colors of the nebulae is required. The spectral energy distribution of the scattered radiation depends upon the absorption coefficient and the scattering efficiency, or albedo, of the particles in the nebulae. We should like to evaluate these physical properties from observations

[1] National Research Fellow at the Yerkes Observatory, 1937–1939.

of the colors of the nebulae, since they depend on the intrinsic properties of the material and might serve to define more closely the nature of interstellar matter. The radiation from the stellar source traverses part of the nebula before it is scattered by a particle, and the scattered radiation must similarly pass through a portion of the nebula before reaching the observer or being scattered a second time. The bluing by scattering is, therefore, counteracted by the reddening by transmission. As we shall see, the two effects may sometimes completely neutralize each other, and the nebula as a whole may have the same color as the illuminating star. We find that the surface brightness is not a simple linear function of the total absorption coefficient, and that for a large optical thickness the brightness is insensitive to variations of the absorption coefficient. This saturation effect can be neglected only when the nebulous sheet is optically thin. Furthermore, since it is necessary to compare the color of the nebula with that of the star, any partial obscuration of the star by nebulous material will produce an additional bluing of the nebula relative to the star.

The dependence of the albedo upon wave length, if present, introduces further complications. The intensity of radiation which has been scattered n times is proportional to the nth power of the albedo. If scattering of higher orders is important, the surface brightness is very sensitive to changes in the albedo. This has been shown to be true[2] when the albedo is large and when the optical thickness of the nebula is great. Although we have no evidence as yet of changes of albedo with wave length, the theoretical aspects are of interest, since any slight variation may become greatly exaggerated.

We shall show how we can disentangle the color effects which are of physical interest from those which depend only upon the fact that we do not observe a single particle but a large ensemble of particles. In addition, we have computed the pertinent optical properties of various types of small particles: the extinction coefficient, the albedo, and the phase function. These results are based upon the classical Mie theory of scattering by small spherical particles. Studies of nebular color should determine whether the matter in the nebulae is in fact similar to that in interstellar space. A determination of the

[2] Henyey, *Ap. J.*, in press.

intrinsic albedo of the nebulous material should be decisive as to the possibility of the existence of metallic particles in space. It is hoped that the results of the following discussion can be applied to the interpretation of recent work on the illumination and color of the nebulae. Studies of the colors of some reflection nebulae have already been made by Yerkes investigators.[3] The recent development of the fast nebular spectrograph[4] will also permit spectrophotometric investigations of the relative intensity of nebula and star over a wide range of wave lengths. The formal theory of nebular illumination will, therefore, aim to derive the intensity of the nebula compared with that of the illuminating star, as a function of wave length, optical thickness, albedo, and geometrical configuration.

FORMAL THEORY

The illumination of a nebula as a whole depends considerably upon the geometrical configuration of the nebulous material and the illuminating source. Since the nebulae are irregular in character, it is necessary to introduce various idealizations in the nature of specific models, and the extreme irregularity of nebulous material is sufficient justification for the study of only the simplest models. The choice of models is not arbitrary, but can be made in such a manner as to represent the essential features of any actual nebula. For instance, there is a fundamental difference between the case of the illuminating star in front of the nebulosity and that of the star behind part or all the material, since the brightness and color of the object are very different in the two cases. We shall consider a homogeneous, plane-parallel slab, viewed from either side, with the star at a great distance from the nebula; we shall also investigate the case of a star at the center of a homogeneous sphere of nebulous material. For a partial representation of the irregularities in space density we shall discuss a model consisting of two plane-parallel slabs lying at different distances from the star. A transition case, that of a star close to the front surface of a nebula, also will be in-

[3] Struve, Elvey, and Keenan, *Ap. J.*, **77**, 274, 1933; Struve, Elvey, and Roach, *Ap. J.*, **84**, 219, 1936; Collins, *Ap. J.*, **86**, 529, 1937; Greenstein, *Ap. J.*, **87**, 581, 1938.

[4] Struve, *Ap. J.*, **86**, 613, 1937; **87**, 559, 1938; Greenstein and Henyey, *Ap. J.*, **86**, 620, 1937; **87**, 79, 1938.

vestigated. The direction from which the nebula is viewed introduces effects of secondary importance[5] that are avoided by considering a mean value of the intensity and color. The actual part of the nebula which we shall consider is its brightest portion.

The first model is a nebula with plane-parallel stratification, illuminated by parallel radiation. We neglect the variation of stellar intensity with distance within the nebula, assuming that the star is at a large distance from the nearest surface. We restrict our attention to the brightest point of the nebula, at which radiation is perpendicularly incident. The diffusion of light at a point in a nebula is governed by the equation of transfer. Using the notation adopted by Henyey,[2] the equation, in terms of specific intensity, I, becomes

$$\cos\theta \frac{dI}{d\tau} + I = \int I\Phi dw + \frac{E}{r^2} e^{-\tau} \Phi . \qquad (1)$$

The energy received from the star at the front surface of the nebula is E/r^2, or $4\pi S$, in ergs/cm^2/sec, where we shall assume that the distance, r, is constant throughout the nebula. The optical depth, τ_λ, depends upon the depth, z, measured inward, perpendicular to the planes of stratification. τ_1 is the total optical thickness of the nebula. The mean value of the intensity, J, satisfies the differential equation[2]

$$\frac{d^2J}{d\tau^2} - p^2 J = -(3 - p^2) \frac{E}{4\pi r^2} e^{-\tau} = -(3 - p^2) S e^{-\tau} . \qquad (2)$$

The quantity p is defined by the relation

$$p^2 = 3(1 - \gamma)(1 - \gamma g) , \qquad (2')$$

where g is a parameter describing the degree to which light is scattered forward or backward relative to the direction of the incident radiation, and where γ is the albedo, or scattering efficiency. The factor $e^{-\tau}$ measures the extinction of the stellar radiation in its passage through the nebula. The net flux, πF, computed with re-

[5] Henyey, *Ap. J.*, **85**, 107, 1937.

spect to the positive z-direction, can be obtained from the solution of equation (2) by means of

$$F = \frac{4\gamma g}{1 - \gamma g} Se^{-\tau} - \frac{4}{3(1 - \gamma g)} \frac{dJ}{d\tau} . \tag{3}$$

The general solution of (2) is given by

$$\frac{J}{S} = Ae^{p\tau} + Be^{-p\tau} + \frac{3 - p^2}{p^2 - 1} e^{-\tau} . \tag{4}$$

There are special forms of the solution when $p = 1$ ($\gamma = \frac{2}{3}$) and when $p = 0$ ($\gamma = 1$), obtained either by taking limiting values of the solution we have given or directly from the simplified forms of the differential equation. The net flux, obtained by means of (3). is

$$\frac{F}{S} = \frac{4}{3(1 - \gamma g)} \left[-pAe^{p\tau} + pBe^{-p\tau} + \left(3\gamma g + \frac{3 - p^2}{p^2 - 1} \right) e^{-\tau} \right]. \tag{5}$$

To evaluate the constants of integration, A and B, we introduce the customary boundary conditions appropriate to the order of approximation here employed. They are

$$\left.\begin{aligned} 2J + F &= 0 , \quad \text{at} \quad \tau = 0 ; \\ 2J - F &= 0 , \quad \text{at} \quad \tau = \tau_1 . \end{aligned}\right\} \tag{6}$$

The determination of the constants in the general case leads to rather involved expressions. As a preliminary step we give the solution for a symmetrical phase function, $g = 0$. The two equations (6) lead to two conditions sufficient to determine A and B; the values of A and B are

$$\left.\begin{aligned} A &= \frac{1}{3} \frac{3 - p^2}{p^2 - 1} \frac{5 \left(1 - \frac{2p}{3} \right) e^{-p\tau_1} - \left(1 + \frac{2p}{3} \right) e^{-\tau_1}}{\left(1 + \frac{2p}{3} \right)^2 e^{p\tau_1} - \left(1 - \frac{2p}{3} \right)^2 e^{-p\tau_1}} , \\ B &= \frac{1}{3} \frac{3 - p^2}{p^2 - 1} \frac{\left(1 - \frac{2p}{3} \right) e^{-\tau_1} - 5 \left(1 + \frac{2p}{3} \right) e^{p\tau_1}}{\left(1 + \frac{2p}{3} \right)^2 e^{p\tau_1} - \left(1 - \frac{2p}{3} \right)^2 e^{-p\tau_1}} . \end{aligned}\right\} \tag{7}$$

These values of the constants, substituted in (4), give J at each point in the nebula. In particular, we are interested in the values of the relative intensity of the nebula and the star, $\mathcal{J}$, at the two surfaces. For the surface facing the star, $\tau = 0$, and we have

$$\mathcal{J}_f = \frac{J(0)}{S} = A + B + \frac{3 - p^2}{p^2 - 1}. \tag{8}$$

Similarly, at the back surface, $\tau = \tau_1$, and we have

$$\mathcal{J}_b = \frac{J(\tau_1)}{Se^{-\tau_1}} = \left(Ae^{p\tau_1} + Be^{-p\tau_1} + \frac{3 - p^2}{p^2 - 1} e^{-\tau_1} \right) e^{\tau_1}. \tag{9}$$

After the substitution of A and B, and simplification, these expressions become, for the star in front of the nebula,

$$\mathcal{J}_f = \frac{2(3 - p^2)}{p^2 - 1} \frac{p \cosh p\tau_1 + (2p^2 - 3) \sinh p\tau_1 - pe^{-\tau_1}}{12p \cosh p\tau_1 + (4p^2 + 9) \sinh p\tau_1}, \tag{10}$$

and for the star behind the nebula,

$$\mathcal{J}_b = \frac{2(3 - p^2)}{p^2 - 1} \frac{5p \cosh p\tau_1 + (2p^2 + 3) \sinh p\tau_1 - 5pe^{\tau_1}}{12p \cosh p\tau_1 + (4p^2 + 9) \sinh p\tau_1}. \tag{11}$$

The mean intensity of the nebular radiation is always referred to the stellar radiation at the surface in question. The intensity of the stellar radiation is S at the front surface, but is $Se^{-\tau_1}$ after extinction within the nebula, when observed at the back surface. Since τ_1 and γ may depend on wave length, it is obvious that $\mathcal{J}_f$ and $\mathcal{J}_b$ give the relative intensity of nebula and star as a function of wave length.

For large values of the optical thickness we obtain the asymptotic expressions

$$\mathcal{J}_f \to \frac{6\gamma}{2 - 3\gamma} \frac{p - 1}{2p + 3} \tag{10'}$$

and

$$\mathcal{J}_b \to \frac{6\gamma}{2 - 3\gamma} \left(\frac{p + 1}{2p + 3} - \frac{10p}{(2p + 3)^2} e^{(1-p)\tau_1} \right). \tag{11'}$$

From this equation we see that if $p < 1$, or $\gamma > \frac{2}{3}$,

$$\mathcal{J}_b \to \frac{60\gamma p}{(3\gamma - 2)(2p + 3)^2} e^{(1-p)\tau_1}, \tag{11''}$$

which approaches infinity. When $p > 1$, or $\gamma < \frac{2}{3}$, we have

$$\mathcal{J}_b \to \frac{6\gamma}{2 - 3\gamma} \frac{p + 1}{2p + 3}. \tag{11'''}$$

The fact that $\mathcal{J}_f$ approaches a constant value in (10′) illustrates the effect of the saturation of the nebular radiation; the nebular intensity approaches a maximum value for large τ_1, and is therefore not dependent on variations of τ_1 with wave length. In equation (11″), when $\gamma > \frac{2}{3}$, we see the effect of the spurious bluing of the nebula relative to the reddened star. It should be noted that equation (11‴) is not the correct representation of the physical problem. A more rigorous investigation shows that the spurious bluing of the nebula is also present for $\gamma < \frac{2}{3}$. The use of the Eddington approximation and the boundary conditions adopted are not justified when the albedo is small and the optical thickness is large. In these cases the dependence of the intensity, I, on angle, θ, in the deep interior of the nebula is such that the approximations are no longer valid.

We shall treat the variation of intensity resulting from variation of τ_1 separately from that depending on γ. Equations (10) and (11) can be differentiated logarithmically with respect to τ_1, to obtain the variation of $\mathcal{J}$ on a logarithmic or magnitude scale. We have computed the logarithmic derivatives given in Figures 1 and 2 for both the front and the back surfaces of the nebula, for albedos $\gamma = 1$, $\frac{5}{6}$, $\frac{2}{3}$, and $\frac{1}{2}$. To obtain the variation of intensity with wave length, we make use of the formula

$$\frac{\partial \log \mathcal{J}}{\partial \log \lambda} = \frac{\partial \log \mathcal{J}}{\partial \log \tau_1} \frac{d \log \tau_1}{d \log \lambda} = \frac{\partial \log \mathcal{J}}{\partial \log \tau_1} \frac{d \log k}{d \log \lambda}. \tag{12}$$

If it is possible to express the extinction coefficient, k_λ, in terms of wave length as

$$k_\lambda \propto \frac{1}{\lambda^n}, \tag{13}$$

we find that

$$\frac{\partial \log \mathcal{J}}{\partial \log \lambda} = -n \frac{\partial \log \mathcal{J}}{\partial \log \tau_1}. \qquad (13')$$

Observations[6] have shown that (13) gives the variation of the interstellar extinction coefficient when n is of the order of unity. If the

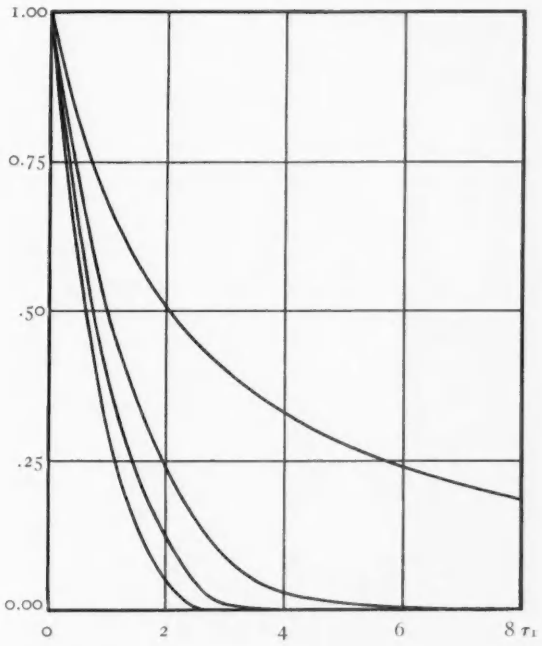

FIG. 1.—Color factor as function of optical thickness for front surface of nebula. From top to bottom the curves correspond to values of the albedo, 1, $\frac{5}{6}$, $\frac{2}{3}$, $\frac{1}{2}$.

color factor, $\partial \log \mathcal{J}/\partial \log \tau_1$, is positive, the nebula is bluer than the star by

$$-0^{m}.24 \times \frac{\partial \log \mathcal{J}}{\partial \log \tau_1}, \qquad (13'')$$

on the international scale of color indices. At the front surface the color factor is less than unity and approaches zero as the optical thickness increases—a result of the saturation effect. For small

[6] Greenstein, *Ap. J.*, **87**, 151, 1938.

albedos the saturation effect becomes of importance at lower optical thicknesses. The color factor at the back surface shows a different behavior. The star is observed reddened through the nebulous material, giving rise to an artificial bluing of the nebula when referred to the star. This fundamental difference in behavior will prove to be of importance in the interpretation of colors of nebulae that are much bluer than the illuminating star—for example, NGC 2068 and

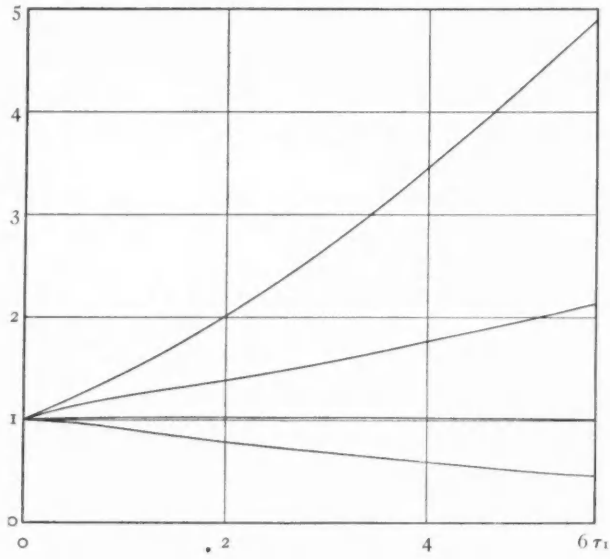

FIG. 2.—Color factor as function of optical thickness for back surface of nebula. From top to bottom the curves correspond to values of the albedo, 1, $\frac{5}{6}$, $\frac{2}{3}$, $\frac{1}{2}$.

2071, as measured by Collins.[3] When $\gamma < \frac{2}{3}$, the color factor as given in Figure 2 apparently decreases with increasing τ_1. For small τ_1 the color factors are roughly correct as given. They are incorrect for large τ_1, since a more exact treatment shows that the color factor eventually increases with τ_1. This arises from the failure of the Eddington approximation, as discussed above. The practical importance of these cases is small, since nebulae of low albedo and great optical thickness would be of very low surface brightness, when observed at the rear surface.

We have assumed in these derivations that the phase function is symmetrical, that is, $g = 0$. We can solve equations (4), (5), and (6)

for $g \neq 0$, for the intensity at the front surface. We introduce the parameters γ', α, and β, defined by

$$\left.\begin{aligned} p^2 &= 3(1-\gamma') = 3(1-\gamma)(1-\gamma g)\,, \\ \alpha &= 1 - \frac{2p}{3}\frac{1-\gamma}{1-\gamma'}\,, \\ \beta &= 1 + \frac{2p}{3}\frac{1-\gamma}{1-\gamma'}\,. \end{aligned}\right\} \tag{14}$$

We then find by the conventional method that $\mathcal{J}_f$ is equal to

$$\frac{3\gamma'}{2-3\gamma'} + \frac{(4\gamma - 9\gamma')(\alpha e^{-p\tau_1} - \beta e^{p\tau_1}) + (\alpha - \beta)(3\gamma' - 4\gamma)e^{-\tau_1}}{(2-3\gamma')(\alpha^2 e^{-p\tau_1} - \beta^2 e^{p\tau_1})}\,. \tag{15}$$

The logarithmic derivative of this expression has been computed for $\gamma = 1$ and $\gamma = \frac{2}{3}$, for $g = +\frac{1}{3}$ and $g = -\frac{1}{3}$. The results are given in Figure 3, for $\gamma = 1$, together with the curve for $g = 0$, for comparison. The effect of positive g (forward-throwing phase function) is to decrease the surface intensity and to shift the incidence of the saturation effect to larger optical thicknesses; the nebulae are, therefore, bluer than for $g = 0$. A negative g has opposite effects. For $\gamma = \frac{2}{3}$ the results are found to be similar but less pronounced. The solutions are, therefore, not sensitive to g.

The conventional boundary-value approximations are known to be sufficient to determine the order of magnitude of the intensity of the nebular radiation. Since the color represents a differential effect, it is desirable to investigate more closely the validity of the approximations. The basis for a second approximation, when the phase function is uniform, is the integral equation for $J(\tau)$, the mean intensity at a point, τ, in the interior of the nebula:

$$J(\tau) = \frac{\gamma}{2}\int_0^{\tau_1} (J(\tau') + Se^{-\tau'})Ei|\tau' - \tau|\,d\tau'\,. \tag{16}$$

The integration of the term in $Se^{-\tau'}$ yields the first-order scattered light corresponding to the Seeliger equation.[5] After substituting the value of $J(\tau')$ derived from our first approximation to the diffuse radiation in equation (4), and integrating, we obtain a second ap-

proximation. The evaluation of the second approximation provides a check of the boundary conditions. For a uniform phase function

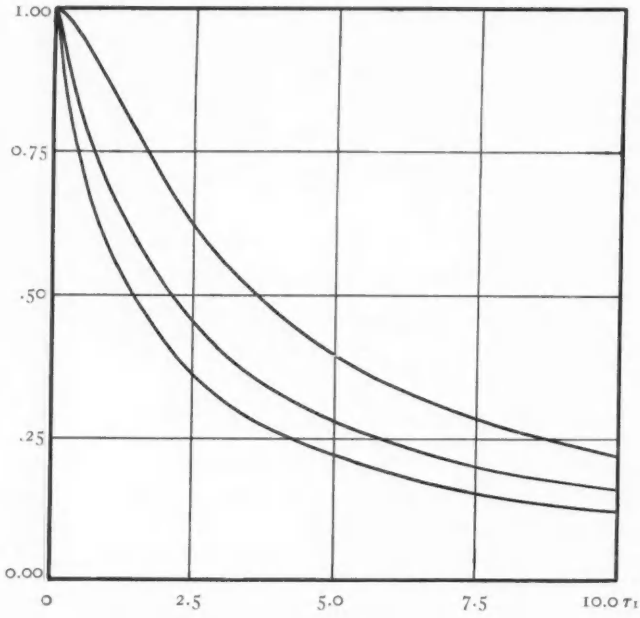

FIG. 3.—Color factor as function of the optical thickness for front surface of nebula, in the case where the albedo is unity. From top to bottom the curves correspond to the asymmetry parameter, $g = +\frac{1}{3}, 0, -\frac{1}{3}$.

and for the plane-parallel model, at the front surface of the nebula, we obtain finally the second approximation,

$$\mathcal{J}_f^* = \frac{J^*(0)}{S} = \frac{\gamma}{2}\left[\frac{2G(-1, \tau_1)}{2 - 3\gamma} + AG(p, \tau_1) + BG(-p, \tau_1)\right], \quad (17)$$

where the functions $Ei(x)$ and $G(a, x)$ are defined by

$$\left.\begin{aligned} Ei(x) &= \int_x^\infty \frac{e^{-u}}{u}\, du\,, \\ G(a, x) &= \int_0^x e^{au} Ei(u)\, du = -\frac{1}{a}\log|1 - a| \\ &\qquad + \frac{e^{ax}}{a} Ei(x) - \frac{1}{a} Eix(1 - a)\,. \end{aligned}\right\} \quad (17')$$

In Table 1 we give the resulting second approximation, computed for unit albedo. We also give the value of $\mathcal{J}_f$ obtained from the usual approximation in equation (10). The table also contains the logarithmic derivatives of $\mathcal{J}_f^*$ and $\mathcal{J}_f$. It will be seen that the first approximation is too low for small τ_1 and too high for large τ_1. The differences, however, are small, and the error is less than 10 per cent in the extreme case. The logarithmic derivatives, or color factors, show only small differences, and it is reasonable to conclude that the

TABLE 1

COMPARISON OF FIRST AND SECOND APPROXIMATIONS TO THE NEBULAR RADIATION

τ_1	$\mathcal{J}_f$	$\mathcal{J}_f^*$	$\frac{\partial \log \mathcal{J}_f}{\partial \log \tau_1}$	$\frac{\partial \log \mathcal{J}_f^*}{\partial \log \tau_1}$
0^m5	0.40	0.43	0.86	0.82
1.0	0.68	0.67	.75	.64
1.5	0.88	0.83	.59	.55
2.0	1.03	0.96	.52	.49
2.5	1.14	1.06	.46	.42
3.0	1.24	1.14	.40	.37
4.0	1.36	1.26	.33	.33
5.0	1.47	1.35	.28	.30
6.0	1.55	1.42	.25	.26
10.0	1.71	1.55	.15	.15
∞	2.00	1.81	0.00	0.00

conventional boundary conditions are sufficiently accurate for the present investigation, if the albedo is high.

An interesting feature of the integral equation (16) is that it can be used to investigate the range of validity of the Seeliger type of approximation used heretofore in studies of nebular illumination. The term in $Se^{-\tau'}$ gives the first-order scattered light (the Seeliger approximation), and is proportional to the albedo. The term in $J(\tau')$ takes account of the rescattering of the diffuse nebular radiation, which is itself proportional to the albedo, when γ is small. An integration therefore gives the observed surface intensity as the sum of terms in γ and γ^2. The integration has been carried through numerically for the intensity at the front surface for infinite optical thickness and for $g = 0$. The result is that $\mathcal{J}_f$ may be written as

$$\mathcal{J}_f = 0.345\gamma + 0.190\gamma^2 + \ldots . \qquad (18)$$

It will be seen that even for the moderate albedo of $\frac{1}{2}$, the second-order scattering of diffuse nebular radiation is nearly 30 per cent of the observed total illumination. Hence, the Seeliger approximation is limited in its application to albedos less than $\frac{1}{2}$.

We have assumed in these models that the linear thickness of the nebula is small compared with the distance from the nebula to the star, or, in other words, that the incident radiation from the star is parallel. We can study some of the effects of this assumption by the investigation of a simple model in which the inverse-square variation of the stellar intensity is taken into account. Let us assume that a star is situated near an infinitely thick nebula, in which the extinction coefficient is k per unit distance (unit distance is the linear separation of the star and the front surface of the nebula). We shall observe the nebula at its brightest point, and shall consider the intensity of the surface compared with that of the star at unit distance, $\mathcal{J}_f$. The Seeliger approximation will be used, with γ less than $\frac{1}{2}$. Since the linear distance, r, from the star to a point in the nebula varies, we must write the specific intensity, I, as

$$I = \gamma k S \int_1^\infty \frac{e^{-2k(r-1)}}{r^2}\, dr\,, \tag{19}$$

if we are to include the inverse-square factor. The integration yields, upon the introduction of the second exponential-integral function, $Ei_2(x)$:

$$\mathcal{J}_f = \frac{I}{S} = \gamma k e^{2k} Ei_2(2k), \tag{19'}$$

and the logarithmic derivative is

$$\frac{\partial \log \mathcal{J}_f}{\partial \log k} = 1 + 2k - \frac{2kEi(2k)}{e^{-2k} - 2kEi(2k)}\,. \tag{20}$$

The values of the logarithmic derivative given in Figure 4 show the analogue of the usual behavior for the case of a star in front of a nebula, that is, the bluing of the nebula decreases with increasing absorption coefficient. In this case, since the optical thickness is infinite, the bluing is produced by an interesting new mechanism.

Briefly, the effective linear distance beneath the surface at which the nebular radiation is produced decreases as the absorption coefficient increases. The available stellar intensity, given dominantly by the inverse-square factor, is greatest when the absorption coefficient is highest. The nebula may be considerably bluer than the star, even when it has a great optical thickness. The more exact solutions which we have developed for the plane-parallel model become very complicated if the inverse-square factor is included; they should not

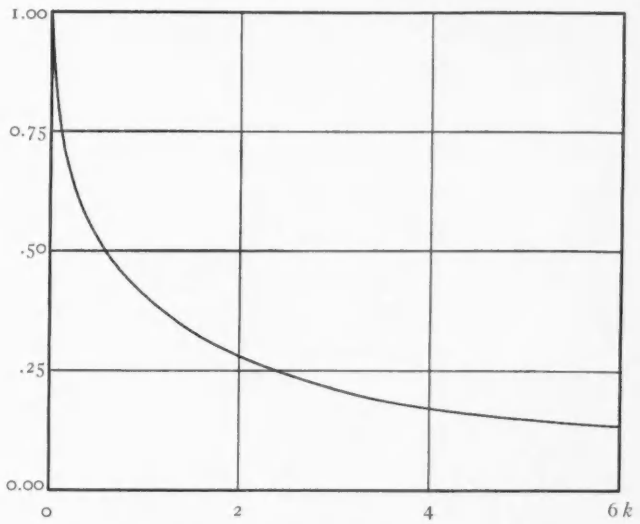

FIG. 4.—Color factor of the first-order intensity at the front surface of a nebula, the linear thickness of which has been allowed for. The color factor is given as a function of the absorption coefficient, k, the unit of distance being taken as the distance between the star and the nebula.

be applied directly if the star is close to the front surface of the nebula.

We have already considered the cases in which the star is well outside of the nebula. To complete the discussion we turn to a model in which the star is completely immersed in nebulosity and in which the inverse-square factor plays a dominant part. Henyey[2] has treated the case of a uniform nebula, spherically symmetrical about the star. He gives the emergent nebular flux, relative to the emergent stellar flux. We have computed the logarithmic derivative of this

quantity for $g = 0$ and for albedos of 1, $\frac{3}{4}$, and $\frac{1}{2}$. In Figure 5 we give the color factor as a function of the radial optical thickness. It can be seen that this model yields essentially the same results as that of the star outside and behind nebulous material. When γ is larger than $\frac{2}{3}$, the nebula becomes much bluer than the star as τ_1 becomes

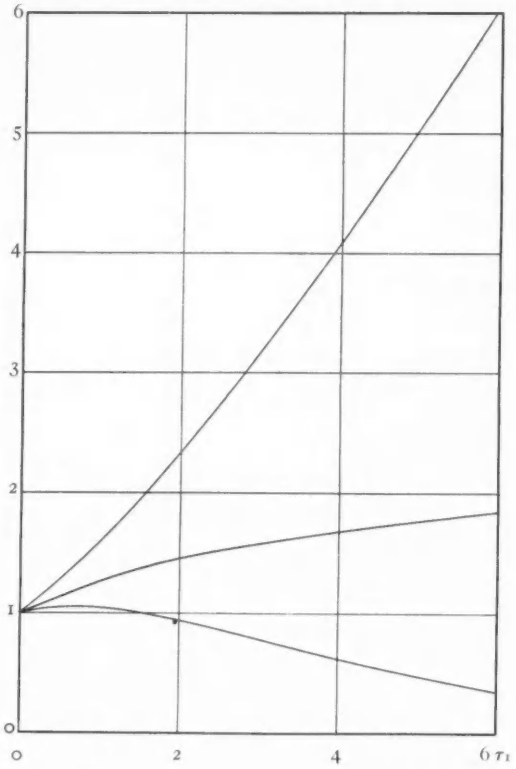

FIG. 5.—Color factor of the emergent flux for a spherical nebula, with the star at the center. From top to bottom the curves correspond to values of the albedo, 1, $\frac{3}{4}$, $\frac{1}{2}$.

large, because of the reddening of the star. The computations for the case of $\gamma = \frac{1}{2}$ give the general trend of the color factor for small τ_1; because of the failure of the Eddington approximation the results are inaccurate for large τ_1. As in the case of the star behind the nebula, shown in equation (11'''), the color factor should properly increase for all albedos. The essential difference produced by the inverse-square factor is that the color factors are, in general, larger

than in the plane-parallel model. The similarity of the results in the two cases when the star is obscured is such as to indicate that the relative color of nebula and star should not be sensitive to the type of model adopted.

We can now complete the discussion by considering roughly the effect of spatial irregularities on the color of the nebula. Let us take two thin parallel slabs of material, viewed from the front, at distances r_1 and r_2 from the illuminating star ($r_1 < r_2$). We consider only the results of the Seeliger approximation. The intensities of the nebular surfaces, for normal incidence and observation, are of the form

$$\left.\begin{aligned} I_1 &= \frac{c}{r_1^2}\left(1 - e^{-2\tau_1}\right), \\ I_2 &= \frac{c}{r_2^2}\left(1 - e^{-2\tau_2}\right)e^{-2\tau_1}, \end{aligned}\right\} \tag{21}$$

where c depends on the phase function and the brightness of the star. The exponential factor $e^{-2\tau_1}$, in the expression for I_2 arises because of the twofold absorption of light by the first nebula. The total observed intensity is the sum of I_1 and I_2, which we shall call I. In many actual nebulae the total obscuration by the dark material is very high, and we have seen that a single sheet of material of great optical thickness can produce little or no bluing. The presence of irregularities, however, permits of color effects even under extreme conditions. Let us suppose that τ_2 is very large, so that the total obscuration in the region approaches infinity. Then we can write I as

$$\frac{I}{c} = \frac{1}{r_1^2}\left(1 - e^{-2\tau_1} + \left(\frac{r_1}{r_2}\right)^2 e^{-2\tau_1}\right). \tag{22}$$

As we vary r_1/r_2, the relative distances from the star of the first nebulous mass and of the thick opaque background of dark material are changed. Figure 6 gives the logarithmic derivative of (22) as a function of τ_1 for various values of r_1/r_2, ranging from $\frac{4}{5}$ in the case when the second nebula is close behind the first to $\frac{1}{5}$ when it is very distant. We see that there is a perceptible color effect, even in the

case of $r_1/r_2 = \frac{2}{3}$. In a nebula that shows fluctuations in space density or filamentary structure, we can expect some color effects even with high total absorption—in the sense that some of the spots may appear blue if they lie closer to the star than does the main body of the obscuring material. While this treatment is based on

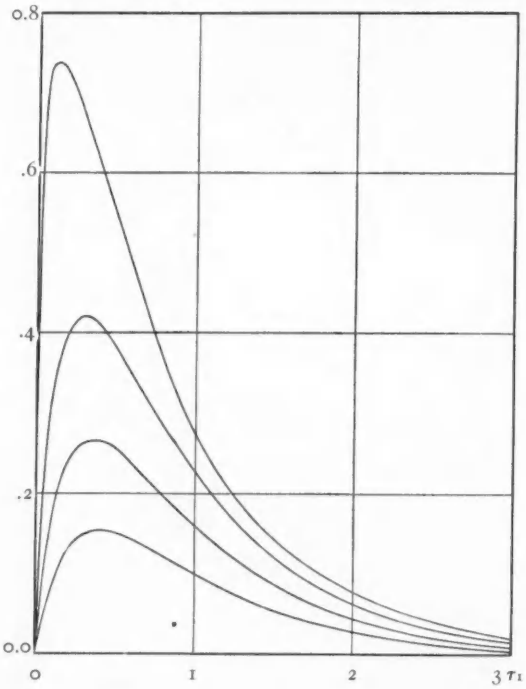

FIG. 6.—Color factor for the first-order intensity in a nebula consisting of a thin sheet of optical thickness, τ_1, superposed on a completely opaque nebula. The curves, from top to bottom, correspond to the cases in which the distance between the star and the thin nebula is $\frac{1}{5}$, $\frac{1}{2}$, $\frac{2}{3}$, $\frac{4}{5}$ of the distance between the star and the opaque nebula.

the Seeliger approximation, it is obvious that the same effects should persist if we were to use the results of the more exact theory.

The possibility of the variation of the albedo with wave length remains, and it will be briefly considered in the case of the plane-parallel model with the star in front of and unobscured by the nebula. It will be assumed that the phase function is uniform, and that the nebula is observed at its brightest point. The solution of the equation of transfer gives, in equation (10), the intensity of the

nebula, $\mathcal{J}_f$, as a function of τ_1 and γ. (It should be remarked that our definition of the albedo is the ratio of the scattering coefficient to the total extinction coefficient of the nebulous material.) The emergent intensity of the nebular radiation is presented in Figure 7, as a function of the albedo, for nebulae of optical thicknesses, $\tau_1 = 1, 3$ and

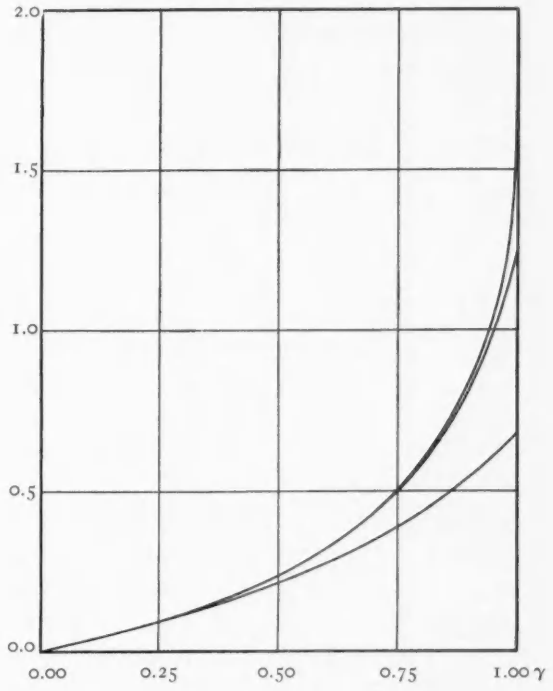

FIG. 7.—The mean intensity of the emergent radiation as a function of the albedo, γ, for the optical thicknesses ∞, 3, and 1, in the order from top to bottom.

$\tau_1 = \infty$. When γ is less than 0.5, the intensity increases linearly with γ, in the range where the first-order scattering predominates; the color factor $\partial \log \mathcal{J}_f / \partial \log \gamma$ is of the order of unity. As γ increases further, the second and higher-order scatterings become important quite abruptly, and the intensity rises very rapidly as the albedo approaches unity. This is particularly striking if the optical thickness is great. It should be noted that the surface brightness of the nebula is very low when γ is small. The rapid increase as γ approaches unity affords an opportunity for determining the albedo

accurately, when the spatial configuration and relative surface brightness of star and nebula are known.

There exists, of course, no analogue of the saturation effect that is found in the variation of the intensity with the extinction coefficient. A change in albedo will always produce a considerable change in the brightness of the nebula, and marked color effects may be expected. A decisive test of the existence of variations of albedo would, therefore, be provided by nebulae whose color differs strongly from that of the star, and in which the color factor, $\partial \log \mathcal{J}_f / \partial \log \tau_1$, could be proved small. Nebulae apparently redder than the star, if peculiar space-absorption effects could be ruled out, also require albedo variations. The matter will be shown to be of particular importance in connection with the existence of metallic particles which have strong variation of albedo with wave length.

PHYSICAL PROPERTIES OF THE NEBULOUS MATERIAL

In studies of the problems of interstellar reddening, much use is made of the classical Mie theory[7] of the scattering and absorption of light by small spherical particles. Scattering and extinction coefficients have been computed for metallic particles by Schalén[8] and by Schoenberg and Jung;[9] for dielectric particles and for mixtures of particles of different sizes, data are given by Greenstein.[10] If it is assumed that the particles in the dark nebulae, with which reflection nebulae are always associated, are similar in composition, size, and frequency distribution to those responsible for interstellar reddening, the available theoretical data are sufficient for the computation of the physical properties necessary in the formal theory of nebular illumination. We shall require the total extinction coefficient, k_λ, the albedo γ_λ, and the asymmetry of the phase function, g. In nebular problems we can investigate the light scattered by small particles as well as the light absorbed, and it is hoped that observations of the nebulae will aid in the solution of the general problem of the interstellar solid material.

The interstellar extinction coefficient is found[6] to vary with wave

[7] *Ann. d. Phys.* **25**, 377, 1908.

[8] *Upsala Medd.*, No. 58, 1933; No. 64, 1935.

[9] *A.N.*, **253**, 261, 1934.

[10] *Harvard Circ.*, No. 422, 1938.

length closely as λ^{-1}. Such a variation can be accounted for by metallic particles of radii 250–500 A, or by a mixture of particles of almost any substance, of a wide range of sizes. The latter hypothesis, supported by the observational evidence for the existence of interstellar hyperbolic meteors, will be considered here in more detail. Let us assume that the number of particles, $N_i(a)$, of radius a and substance i, is given by the frequency function

$$N_i(a) = N_i a^{-s} . \tag{23}$$

We obtain the integrated extinction coefficient for such a mixture, $\bar{k}_\lambda$, as

$$\bar{k}_\lambda = \pi N_i \int_{a_1}^{a_2} a^{2-s} Q_\lambda(a) da , \tag{24}$$

where $Q_\lambda(a)\pi a^2$ is the cross-section for extinction given by the Mie theory. If we transform to the variable, α, given by

$$\alpha = \frac{2\pi a}{\lambda} ,$$

we obtain

$$\bar{k}_\lambda = \pi N_i \left(\frac{\lambda}{2\pi}\right)^{3-s} \int_{\alpha_1}^{\alpha_2} \alpha^{2-s} Q(\alpha) d\alpha , \tag{24'}$$

where $Q(\alpha)$ is not a function of wave length for dielectrics. An interesting schematic representation can be obtained if we assume that $\alpha_2 \to \infty$ and $\alpha_1 \to 0$, that is, that particles of all sizes are present. The integral in (24′) is then a constant, K_i, calculable from the Mie theory by a numerical integration, and the total extinction is given by

$$\bar{k}_\lambda = \pi N_i K_i \left(\frac{\lambda}{2\pi}\right)^{3-s} . \tag{25}$$

If $s = 4$, the extinction coefficient will vary as λ^{-1}. It is interesting to note that the larger interstellar dust particles, represented by the hyperbolic meteors,[11] have just such a frequency distribution, with

[11] Öpik, *Harvard Circ.*, No. 359, 1931; Watson, *Harvard Ann.*, **105**, No. 32, 1937.

s between 3.3 and 4.2. For both metallic and dielectric particles we can evaluate the integrals K_m and K_d. For metals K_m varies slightly with wave length, depending upon the optical properties of the metal; a further question which arises is that if $s \geq 4$, K_m becomes infinite when a_1 approaches zero. Since we must restrict ourselves to particles larger than a few atoms, this difficulty is trivial; values of the integrals are computed by Greenstein.[10]

Observational evidence and the theoretical interpretation seem to justify us in assuming that $\bar{k}_\lambda$ is of the form λ^{-1}, and that $d \log \bar{k}_\lambda / d \log \lambda$ is of the order of -1 in interstellar space and probably in the nebulae. An infinitely thin nebula, with the star in front, should then be bluer than the star by the λ^{-1} factor, which is -0.24 mag. on the international scale, if the albedo is held constant. Investigations with the new nebular spectrograph at the McDonald Observatory are planned to determine the energy distribution in the spectra of some reflection nebulae.

The albedo of the particles, as used in the formal theory, is given by the ratio of the scattering coefficient, k'_λ, to the total extinction coefficient, k_λ. For purely dielectric substances there is no consumptive absorption (production of Joule heat), so that the scattered light is equal to the light loss of the incident radiation and the albedo is always unity. Metallic particles possess a considerable consumptive absorption, and the scattering coefficient is only a part of the total extinction coefficient. The albedo is less than unity for large particles (of the order of the reflectivity of the bulk metal), has a maximum near $a = 1$, and becomes very small for particles small compared to the wave length. Since particles of the latter type have been suggested as the source of the space reddening, their low albedo affords an interesting test of their existence in the nebulae.

The albedo of metallic particles can be derived from the Mie theory:

$$\gamma_\lambda = \frac{k'_\lambda}{k_\lambda} - \frac{\sum_{n=1}^{\infty} \frac{|a_n|^2 + |p_n|^2}{2n+1}}{\text{Imag. part} \sum_{n=1}^{\infty} (-1)^n (a_n - p_n)} . \qquad (26)$$

Schalén gives values of the quantities a_n and p_n, the amplitudes of the partial scattered waves, computed from the Mie theory. It is therefore possible to compute γ_λ for various metallic substances, as a function of particle radius, a, and refractive index, μ_λ. When the particles are small compared with the wave length of light ($a < 1$), it can be shown that a good approximation to the albedo is given by

$$\gamma_\lambda = -\tfrac{2}{3}\, a^3 \frac{\left|\dfrac{\mu_\lambda^2 - 1}{\mu_\lambda^2 + 2}\right|^2}{\text{Imag. part}\left(\dfrac{\mu_\lambda^2 - 1}{\mu_\lambda^2 + 2}\right)}. \qquad (27)$$

The albedo for metals is therefore much less than unity, when a is less than unity; the theory of interstellar reddening requires that

TABLE 2

ALBEDOS OF METALLIC PARTICLES

Radius a in Angstroms	Iron			Nickel		
	$\lambda = 3950$ A	$\lambda = 4400$ A	$\lambda = 5500$ A	$\lambda = 3950$ A	$\lambda = 4400$ A	$\lambda = 5500$ A
100	0.0032	0.0026	0.0017	0.0082	0.0081	0.0063
200	.026	.021	.013	.067	.066	.051
300	.086	.070	.046	.22	.22	.17
500	.....	.20	.15	.44	.49	.41
1000	.45	.42	.44	.46	.58	.69
1750	0.51	0.49	0.51	0.48	0.67	0.71
Bulk	0.26	0.28	0.31	0.50	0.56	0.64

$a < 1$. Table 2 gives γ_λ for iron and nickel at various wave lengths and for a range of particle sizes (given in Angstrom units). The reflectivity of the bulk metal is given, for comparison, in the last row of the table. The metallic albedos are usually less than $\frac{1}{2}$; in the range of particle sizes suggested for interstellar reddening they vary from 0.002 to 0.49, depending on the radius and the optical constants of the substance. The dependence upon wave length also changes with particle size.

We can investigate the properties of a mixture of metallic and dielectric particles of a wide range of radii. Let us assume that the frequency functions are the same for a dielectric substance and for a

metal, with abundances by volume, N_d and N_m, respectively. The frequency functions are, then,

$$N_d(a) = N_d a^{-s},$$
$$N_m(a) = N_m a^{-s}.$$

We can compute the integrated albedo, $\bar{\gamma}_\lambda$, of such a mixture as a function of the relative abundance of metallic and dielectric particles, N_m/N_d. The necessary integrals for the total extinction, K_d and K_m, are obtainable when $Q(a)$ is known; the values of $Q(a)$ given in *Harvard Circular*, No. 422, have been used. The integrated scattering coefficient is given by

$$\bar{k}'_\lambda = \pi N_i \left(\frac{\lambda}{2\pi}\right)^{3-s} \int_0^\infty a^{2-s} Q(a)\gamma(a)da\,, \tag{28}$$

where $\gamma(a)$ is obtainable from our Table 2. The effective albedo is

$$\bar{\gamma}_\lambda = \frac{\bar{k}'_d + \bar{k}'_m}{\bar{k}'_d + \bar{k}_m}. \tag{29}$$

Table 3 gives the resulting effective albedo at two extreme wave lengths, as a function of relative abundance. The dielectric substance adopted is a perfect reflector ($\mu = \infty$); the particles are assumed to have a lower limit of radius at 10 A; the frequency constant, s, is taken as 4. Such a mixture would have an extinction coefficient that would vary as λ^{-1}. The integrated albedos, when only metallic particles are present, range between 0.13 and 0.56, and are larger in the red than in the violet.

If the interstellar particles prove to have low albedos, a variation of albedo with wave length might be expected. Present estimates of the albedo are not sufficient for a decisive test of the type of substance present, and further observations are being planned in this connection. The values of the albedo suggested by the available data[12] lie between 0.1 and 0.7, and the high intensity of the diffuse illumination of the Milky Way indicates even larger albedos.[13]

[12] Struve, *op. cit.*, **85**, 194, 1937.

[13] Elvey and Roach, *Ap. J.*, **85**, 213, 1937; Henyey, *Ap. J.*, **85**, 255, 1937.

A further quantity necessary in the formal theory of nebular illumination is the asymmetry of the phase function for small par-

TABLE 3

EFFECTIVE ALBEDO OF MIXTURES OF METALLIC AND DIELECTRIC PARTICLES

N_m/N_d	Iron		Nickel	
	$\lambda = 4000$ A	$\lambda = 6300$ A	$\lambda = 4000$ A	$\lambda = 6300$ A
0.00	1.00	1.00	1.00	1.00
0.01	0.96	0.96	0.97	0.99
0.05	0.83	0.85	0.89	0.95
0.10	0.71	0.75	0.81	0.91
0.25	0.52	0.57	0.67	0.82
0.50	0.38	0.43	0.56	0.74
0.75	0.30	0.36	0.51	0.71
1.0	0.27	0.32	0.48	0.68
2.0	0.21	0.24	0.46	0.66
∞	0.13	0.15	0.36	0.56

TABLE 4

THE ASYMMETRY OF THE PHASE FUNCTION

Substance	Particle Radius a	Asymmetry g
Dielectric ($\mu = 1.25$)	0.01	+0.00
	0.8	+ .10
	1.6	+ .47
	4.0	+ .96
	8.0	+ .99
Metal ($\mu = 0.75 - 2.45i$)	0.91	+ .22
	1.03	+ .33
Euler phase function	Very large	− .33
Lambert phase function	Very large	−0.44

ticles. If $(\pi - \theta)$ is the angle between the incident and the scattered ray, the quantity g is defined as[2]

$$g = \frac{\int_0^\pi I(\theta) \sin \theta \cos \theta d\theta}{\int_0^\pi I(\theta) \sin \theta d\theta} . \qquad (30)$$

If the distribution of intensity, $I(\theta)$, is known as a function of θ, the asymmetry can be determined. For particles of radius near the wave length of light, $I(\theta)$ is available in computations by Blumer[14] based on the Mie theory. Blumer and Mie give phase diagrams and tables of $I(\theta)$ for particles of various sizes and refractive indices. A numerical evaluation of the integrals in (30) give the values of g found in Table 4. Particles that have the greatest mass-scattering coefficients ($a \approx 1$) have positive values of g, i.e., the light is thrown dominantly forward. The conventional phase functions for large particles (Euler or Lambert) have negative g; the light is thrown backward and the particle casts a shadow. The large values of g when $a \approx 1$ indicate that g must be positive and rather large for particles responsible for most of the nebular scattering. The types of approximation used in the solution of the equations of radiative transfer are not accurate if g lies outside the range $-\frac{1}{3}$ to $+\frac{1}{3}$. A more complete treatment for extremely asymmetrical phase functions, however, would probably not reveal any essentially novel features; the effect of g is found predominantly in the shape of the nebula.

YERKES OBSERVATORY
June 1938

[14] *Zs. f. Phys.*, **32**, 119, 1925; **38**, 305, 920, 1926.

THE TEMPERATURES OF THE EXTRAGALACTIC NEBULAE AND THE RED-SHIFT CORRECTION*

JESSE L. GREENSTEIN

ABSTRACT

The spectral energy distribution in nebulae can be measured with the new nebular spectrographs at the Yerkes and McDonald observatories. The mean energy-curve (based on seven plates) of the Andromeda nebula relative to stars of known color temperature is given in the figure. From λ 6500 to λ 3900 it closely resembles that of a black body of temperature 4200°. A calibration of temperatures from color indices is therefore justified. The mean color temperature of the nebulae lies between 4700° and 5250°. The effect of such low temperatures on the present interpretation of the counts of extragalactic nebulae is serious. It seems improbable that the effect of the red shift on the apparent magnitudes of the nebulae, found by Hubble, can be interpreted either as a velocity or as a nonvelocity shift. The effect of absorption lines, and of a possible ultraviolet excess, on the energy distribution and on the magnitude corrections is briefly investigated.

SPECTROPHOTOMETRY OF NGC 224

Color indices of extragalactic nebulae have been measured photographically in both the yellow and the red color systems, and photoelectrically over a shorter range of wave lengths. The determination of reliable color temperatures from color indices requires some theoretical or observational justification, since the energy distribution in the composite spectrum of a nebula might deviate from that in a black body. Unfortunately, spectrophotometry over a wide range of wave length is difficult with a slit spectrograph; with an objective prism, or slitless spectrograph, the finite diameter of the nebular image provides a serious obstacle.

The new nebular spectrographs described by Struve[1] are well suited to spectrophotometry of diffuse objects. The effects of differential refraction can be neglected; the spectrum can be given almost any desired purity; and, since there is no collimator, the width of the spectrum is controlled solely by the Schmidt camera. While there is some residual chromatic aberration in the $f/1$ Schmidt camera, a tilt of the plateholder makes the width of the spectrum constant from the red to λ 3700. The spectral energy distribution in a star can be accurately determined, therefore, the only condition being

* *Contributions from the McDonald Observatory, University of Texas*, No. 10.

[1] *Ap. J.*, **86**, 613, 1937; Struve, Elvey, and Van Biesbroeck, *ibid.*, **87**, 559, 1938.

that the optical axis of the instrument coincides with the direction of the star. (This condition is not very critical, especially in the case of extended objects such as nebulae.) With the earlier form of the nebular spectrograph at the Yerkes Observatory the comparison of two stellar spectra was subject to considerable accidental error, since it was not possible to check the centering of the star on the prisms. With the spectrograph now in use at the McDonald Observatory the axis from star to slit can be accurately centered on the prisms, and the comparison of nebula and star is theoretically justified. The effect of inaccurate setting is to introduce a vignetting in the prisms and in the camera, which may vary with wave length; it has the effect of an accidental error in the measured gradients, since it changes sign at the position of centering.

The spectrum of the unresolved nuclear region of the Andromeda nebula, NGC 224, has been compared with the spectra of stars of various spectral types for which Greenwich gradients[2] are available. The spectrograph integrates the radiation from an area about 3′ in diameter, equivalent to the central portion of fainter extragalactic nebulae usually photographed. Five plates of the nebula were obtained with the Yerkes nebular spectrograph, as well as seven plates of comparison stars. Two plates were obtained with the McDonald spectrograph, and three plates of the comparison stars. The exposure times on the nebula averaged thirty minutes, and on the stars eight minutes. The laboratory calibrations, with exposures averaging fifteen minutes, were made by a spectral sensitometer, using a platinized wedge kindly provided by Dr. Brian O'Brien. A tube photometer with red and blue filters was also used. Agfa Super Pan Press films gave roughly uniform density in a single exposure over the range from λ 6600 to λ 4000. The rapid decrease of density beyond λ 3900 is such as to require extra exposures for this region, which has consequently not been studied.

The magnitude differences between star and nebula for each exposure were measured on a photoelectric recording microphotometer. Plotted against $1/\lambda$, these differences were very nearly linear within the errors of observation. The mean of the magnitude differences

[2] Greaves, Davidson, and Martin, *Greenwich Pub.*, 1932; *M.N.*, **94**, 488, 1934.

is plotted in Figure 1, which gives the magnitude of the nebula minus the mean of the stars. The spectral types of the comparison stars ranged from B5 to G0, the weighted mean type being F0; the mean Greenwich gradient was 1.52. The deviations from the straight

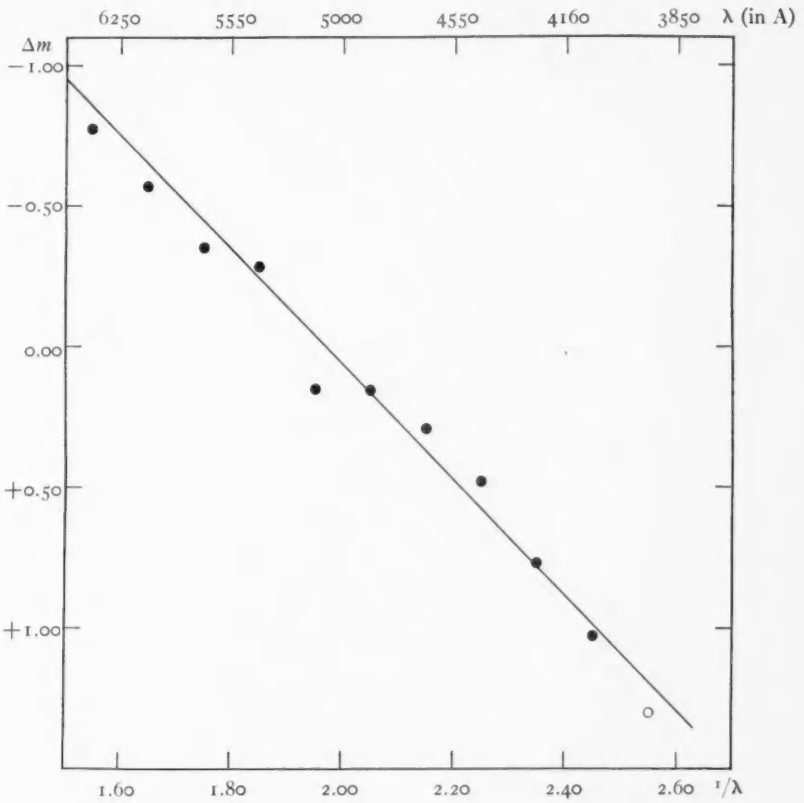

FIG. 1.—The spectral energy distribution in the Andromeda nebula, relative to the mean of the comparison stars. The straight line corresponds to a temperature of 4200°.

line plotted in the figure correspond to a mean error of ±0.07 mag., which is larger than might be expected. The mean error of a magnitude difference from a single pair of plates was ±0.11 mag. Imperfect axial adjustment may be the source of the large accidental errors in the Yerkes spectrograms. A least-squares solution gives the plotted straight line; the slope corresponds to a difference of

gradient of 1.87. The final adopted gradient is 3.39, which yields a color temperature of 4200° ± 200°.

The point at $1/\lambda = 1.95$ (in microns^{-1}) is inaccurate because of the dip in plate sensitivity in the green; line absorption near H and K and the band at λ 3883 cause the points at $1/\lambda = 2.45$ and $1/\lambda = 2.55$ to lie below the curve. These and other absorption lines may be the explanation of the deviations from the straight line. It may be noted that the deviations of the points from the straight line in the figure are in the same sense as in the case of the deviations of the solar energy-curve from a black body. The solar energy-curve shows an excess at λ 4500 and a deficiency at λ 3900. There seems to be no significant departure from linearity of the relative energy-curve of the nebula and stars, over the range from λ 6500 to λ 3900; and we can therefore represent the observed composite spectral energy distribution of the nebula, at least approximately, by a black body of temperature 4200°. The spectral type of the nebula is given as dG5; the line absorption is then stronger than for F0, the mean of the comparison stars. The color temperature here obtained is probably slightly lower than one obtained by comparison of the nebula with stars of the same spectral type, because of the increased strength of the absorption lines in the violet.

TEMPERATURES FROM COLOR INDICES

The color temperature derived above is apparently very low for the spectral type of the nebula. It is confirmed, however, by the photoelectric measures of Stebbins and Whitford,[3] who find the color index, C_2, of NGC 224 to be + 0.12 mag. This value corresponds on their color scale to the color of a star of spectral type dK2: (extrapolated), or gG7. The effective temperatures of such stars[4] are about 4500°, in good accordance with our present value of 4200°. (The relation between effective and color temperatures is discussed below.) Since the nebula is at a low galactic latitude (−20°), it is probable that reddening within our galaxy may account for part of the large color excess. A correction for such reddening on the basis of the cosecant law raises the color temperature to 4400°, or to 4700° from the photoelectric value. There still remains an excess in gradient of +0.59, corresponding to a color excess of

[3] *Ap. J.*, **86**, 247, 1937.

[4] Kuiper, *ibid.*, p. 176.

+0.3 mag. on the international scale. The Andromeda nebula is intrinsically one of the reddest of the extragalactic nebulae.

The large color excess generally observed for nebulae and the low temperature indicated for NGC 224 have important theoretical consequences in the interpretation of the counts and in the space density of extragalactic nebulae. It may therefore be of value to attempt to derive the color temperatures of the nebulae as indicated by the available color indices. The close approach to a black-body curve, indicated in the figure, may be taken as partial justification of the conversion of color indices into temperatures. The data of Stebbins

TABLE 1

MEAN REDDENING IN A UNIFORM ABSORBING MEDIUM

τ_{pg}	Δc International	Δc Photoelectric
$0^m.1$	$0^m.03$	$0^m.01$
0.2	.05	.02
0.4	.08	.03
0.6	.11	.04
1.0	0.28	0.11

and Whitford provide an excellent selection of very accurate colors of nebulae of various structural types, from E to Sc. The quantity we desire is the mean color index of all nebulae (over all galactic latitudes) to a given limiting magnitude. This may be derived from the colors of a selected group of nebulae by correcting the observed colors by means of the cosecant relation to a point outside the galactic reddening material, and by then applying the theoretical mean reddening correction, Δc, given in Table 1. Let τ_{pg} be the optical thickness of the absorbing material in the galaxy at the photographic effective wave length. We will take the optical thickness for reddening, τ_E, to be of the order of $\tau_{pg}/5$ on the international scale and $\tau_{pg}/13$ on the scale of the photoelectric colors, C_2. It can be shown that the mean reddening of the nebulae observed through such a uniform absorbing layer is Δc, given by

$$\Delta c = \frac{\tau_E}{2} \frac{Ei(t)}{e^{-t} - tEi(t)}, \qquad (1)$$

where $Ei(t)$ is the exponential-integral function and

$$t = 0.6\ \tau_{pg} \log_e 10 .$$

The selection of nebulae according to galactic latitude made by the photoelectric observers favored high-latitude objects and only partly balanced the corrections of the last column in Table 1, if we take τ_{pg} to be about 0.5 mag. The adopted mean colors of nebulae of various types, given in Table 2, are derived from the colors given by Stebbins and Whitford in their Table 4, by correcting them for galactic reddening, as described above. Column (3) gives the equivalent spectral type of stars of the same color, and column (4) the effective temperature, *Te*, taken from the data of Kuiper. The color temperatures are derived rather indirectly by means of a calibration[5] of the earlier photoelectric scale of colors, C_1, in terms of Greenwich gradients. Stebbins and Whitford give the relation

$$C_1 + 0^m.10 = 1.68\ (C_2 + 0^m.27) ; \qquad (2)$$

and I have found that my gradients, φ, are given by

$$\varphi = 1.51 + 3.36\ C_1 . \qquad (3)$$

The stars common to the Greenwich list and the catalogue of Stebbins and Huffer[6] yield the relation between Greenwich gradient, φ_{gw}, and C_1 as

$$\varphi_{gw} = 1.40 + 3.08 C_1 . \qquad (4)$$

The mean of the results from equations (3) and (4), together with (2), yield the color temperatures of the nebulae, *Tc*, in column (5). That these are roughly correct is shown by column (6), which contains the spectrophotometric color temperatures obtained by Miss Maulbetsch[7] for dwarf stars. The effective temperatures and the color temperatures agree remarkably well. The last column gives the frequency of the various classifications among nebulae brighter than the thirteenth magnitude.[8]

[5] Greenstein, *ibid.*, **87**, 151, 1938.

[6] *Pub. Washburn Obs.*, **15**, No. 5, 1934.

[7] *Harvard Circ.*, No. 377, 1932.

[8] Shapley and Ames, *Harvard Ann.*, **88**, No. 2, 1932.

There may be some question as to the high temperature indicated for Sc nebulae in Table 2, because of the possible existence of emission lines in the narrow spectral regions used by Stebbins and Whitford. Unpublished investigations by Dr. C. K. Seyfert and the author suggest that the emission lines arising from the diffuse nebulae which occur in late-type spirals may contribute appreciably to the integrated spectrum and color. The determination of color temperatures, *Tc*, from color indices is, in general, rather indirect and does not take full account of the effect of the absorption lines

TABLE 2

TEMPERATURES OF THE NEBULAE

Type	Mean Corrected Color, C_2	Equivalent Spectral Type	*Te*	*Tc* Photo-electric	*Tc* Spectro-photometric	*N*
E	$+0^{m}.09$	dK1	4800°	4700°	4900°	217
Sa	+ .10	dK1	4800	4700	4900	64
Sb	+ .05	dG9	5100	5300	5200	72
Sc	−0.05:	dF7:	6100:	6500:	6200:	156

on the color of the nebula, a point discussed in the next section. The weighted mean effective temperature, *Te*, for all nebulae is 5250°; if the Sc objects are excluded, the mean becomes 4900°. The corresponding values for the color temperatures are 5350° and 4900°. In any case, a mean effective temperature higher than 5250° seems rather improbable.

We may briefly review the temperatures obtainable from the photographic investigations of colors of nebulae. Hubble and Humason[9] and Baade[10] have obtained colors, on the international scale, of a total of 110 nebulae. The corresponding equivalent mean spectral type is G9. Whipple[11] and Seyfert[12] have obtained red color indices for 107 nebulae, which yield an equivalent spectral type of G9. The spectral types are calibrated by means of colors of a mixture of dwarf and giant stars brighter than the eleventh magnitude,

[9] *Ap. J.*, **74**, 43, 1931.

[10] *Mt. Wilson Obs. Report*, 1934.

[11] *Harvard Circ.*, No. 404, 1935.

[12] *Harvard Ann.*, **105**, No. 9, 1937.

so that it is difficult to interpret them in terms of effective temperatures. With an estimate of 40 per cent dwarfs, an effective temperature of 4600° seems reasonable. Details of the selection of the nebulae according to galactic latitude and nebular type are not available, so that no proper reduction to a general mean color can be made.

EFFECT OF THE RED SHIFT ON NEBULAR MAGNITUDES

The observational material for the discussion of the distribution of extragalactic nebulae is given by Hubble.[13] His present observations indicate a dimming of the light of a nebula by the red shift in the amount Δm given by

$$\Delta m = B \frac{d\lambda}{\lambda}, \tag{5}$$

with $B = 2.94$. A part of the dimming of the light when the spectrum is shifted to the red arises from the lower intensity of the portion of the spectrum past the maximum of the spectral energy distribution, which is shifted into the wave-length region in which the nebula is photographed. This part of the dimming is determined by the spectral energy distribution, as weakened by absorption lines, in the composite spectrum of the nebula. We can write the energy-effect term, called $K + \Delta m_E$ by Hubble, as

$$K + \Delta m_E = B^* \frac{d\lambda}{\lambda}, \tag{6}$$

for the small observable red shifts. Δm_E gives the loss of energy by a quantum when shifted to the red, and K depends on the energy distribution in the spectrum. Hubble gives a table of values of K for various black-body temperatures. Table 3 gives the predicted effect of the red shift on the apparent magnitudes of the nebulae, as given by Hubble, together with a new computation for $T_0 = 4500°$.

It can be seen that $B^* - 1 \gtrsim B$ unless T_0 is greater than 5250°. The low mean effective temperature here found for the nebulae

[13] *Ap. J.*, **84**, 517, 1936.

(which agrees with the value given by Hubble in the last column of his Table 7) is such that B^*-1 seems to be, in fact, greater than or equal to B; in this case no proper interpretation of the nebular counts is available. Hubble has shown that

$$\Delta m = B^* \frac{d\lambda}{\lambda} \tag{7}$$

if the red shifts are not velocity shifts, and that

$$\Delta m = (B^* + 1) \frac{d\lambda}{\lambda} \tag{8}$$

if they are velocity shifts. Neither hypothesis is tenable when $B^* \geqslant B$, that is, for T_0 less than 6100°. Even a loss of energy, when a

TABLE 3

RED-SHIFT CORRECTION FOR A BLACK BODY

T_0	B^*
6000°	3.0
5500	3.6
5000	4.5
4500	5.5

photon is shifted to the red, is incompatible with the observations when $B^*-1 \geqslant B$. If the color temperature, or effective temperature, here derived for the nebulae describes a spectral energy distribution similar to that of a black body of the given temperature, this conclusion is inescapable.

The possible deviations from black-body distribution in the nebulae may be investigated by means of the spectral energy distribution of the sun, which has been accurately observed. The nebular spectra are found to be very similar to dwarf G stars with respect to the absorption lines in the photographic region. The irregular distribution of the absorption lines and the variation of the opacity coefficient with wave length make the sun deviate considerably from a black body. By evaluating the magnitude correction, $K + \Delta m_E$, produced by various red shifts, $d\lambda/\lambda$, on the known energy distribution of the sun, we will be able to determine a pseudo-temperature operative in the red-shift magnitude correction. Hub-

ble has made a similar determination of $K + \Delta m_E$ for the sun, but with quite discordant results. The discordance may arise from his reduction of the integrated energy distribution to a point near the limb of the sun. It seems preferable to use the observed integrated energy distribution, obtained spectrobolometrically, which includes the effect of the absorption lines, so as to obtain the most direct and accurate comparison with nebular spectra.

I have computed the response of Eastman 40 plates to radiation after two reflections from silvered mirrors, and after passage through a zenith atmosphere at Mount Wilson. Pettit's values for the ultraviolet energy distribution in integrated sunlight outside the atmosphere were adopted.[14] Table 4 gives the relative magnitudes of the

TABLE 4

RED-SHIFT CORRECTION FOR THE SOLAR SPECTRUM

$d\lambda/\lambda$	K	$K+\Delta m_E$
0.00	$0^m.00$	$0^m.00$
.10	0.29	0.40
.20	0.65	0.84
.25	0.84	1.09
.30	0.99	1.28
0.50	1.92:	2.36:

solar radiation for various red shifts. On fitting the points for $d\lambda/\lambda \leqslant 0.25$, the value of B^* is found to be 4.20. This corresponds, according to Table 3, to the constant B^* for a black body of temperature 5200°. The integrated color temperature of the sun, as determined from the slope of the energy-curve, is known to vary from 6200° in the visual region to less than 5200° in the region from λ 4400 to the ultraviolet. It is apparent that the solar-type spectra of the nebulae would behave (neglecting their color excess) as if they possessed a pseudo-temperature lower than either the effective temperature (5740°) or the visual color temperature. The result is not unexpected, since it is obvious that the low color temperature in the ultraviolet, caused by the great number of absorption lines, is the dominant factor. The nebulae have lower color temperatures

[14] *Ibid.*, **75**, 185, 1932.

than the sun; but we may generalize our results to say that the color temperature, or the effective temperature, of the nebulae are upper limits to the temperature to be used in the computation of the red shift. With the solar distribution of absorption lines the mean temperature of the nebulae might be taken as 4800.°

As far as the spectral distribution of absorption lines is concerned, the spectra of nebulae are not very different from that of the sun. The mean spectral type of the nebulae involved in the photoelectric color temperatures is given as G1.6, and the general mean given by Hubble is G3. The color excess of the nebulae corresponds to a difference in temperature of 500° between that given by the spectral type and by the energy distribution. If the color excess arises from absorption and reddening within the nebula, it will presumably behave like reddening within our own galaxy, which transforms a black-body energy-curve to that of a black body at a lower temperature.[5] (If the absorption varies more rapidly than λ^{-1}, the temperature for red shifts will be lower than the temperature measured in the visual region.)

If the color excess arises from the composite nature of the spectrum of a nebula, as has been suggested by Whipple,[11] the distribution both of absorption lines and of the continuous radiation may differ in the ultraviolet from that in the usual spectral regions. This aspect of the problem is necessarily speculative at present, since it depends on the unknown frequency of luminous hot stars in various nebulae. A rough measure of such an ultraviolet excess may be obtained from an integration of the emission of the stars in our own galaxy, which is probably similar to a late-type spiral and which possesses relatively large numbers of hot stars. Seares states[15] that the late-type spirals possess very luminous blue stars, mainly in their outer regions, so that it seems probable that the ultraviolet excess found for our neighborhood in the galaxy will be an extreme value.

We will assume that the stars radiate like black bodies of color temperature equal to their effective temperature. The conventional luminosity function for stars of various spectral types and absolute magnitudes then yields the monochromatic intensities, I_λ (on an

[15] *Proc. Nat. Acad. Sci.*, **2**, 553, 1916.

arbitrary scale), given in the second column of Table 5. Column (3) gives the black-body distribution for 6000°, for comparison; and column (4) gives the excess energy, in magnitudes, of the composite spectrum over that in a black body. This completely neglects the effect of reddening within the galaxy. To evaluate the reddening, we will adopt the λ^{-1} law for the dependence of the absorption coefficient on wave length. If the albedo of the absorbing particles in interstellar space is unity, then the scattered radiation plus the light of the reddened stars will be observed together, with the same integrated energy distribution as in the case of no absorption, column

TABLE 5

ENERGY DISTRIBUTION FOR THE NEIGHBORHOOD OF THE SUN

λ	I_λ	Black Body 6000°	Excess	I_λ (Abs.)	Black Body 5500°	Excess
3000.....	0.89	0.53	-0^m6	0.67	0.40	-0^m6
4000.....	1.03	0.92	— .1	0.93	0.82	— .1
5000.....	1.00	1.00	.0	1.00	1.00	.0
6000.....	0.96	0.90	— .1	1.03	0.96	.0
7000.....	0.92	0.75	−0.2	1.01	0.83	−0.2

(2). If the albedo is zero, the intensity distribution is altered to I_λ(Abs.), given in column (5), for a mean optical thickness of $\tau_{pg} = 0.5$ mag. and for nebulae of random orientation. Again, for comparison, the black-body distribution for 5500° is given in column (6), and the excess of the composite radiation in the last column. The absorption produces a color excess of 500° in the extreme case of zero albedo; larger values of the optical thickness might be appropriate for the nuclear regions of the nebulae and would produce greater color excess. The ultraviolet excess would persist in any case and can amount to −0.6 mag. at λ 3000. Such an ultraviolet excess of energy should be observable if present.

A rough evaluation may be made of the effect of such an excess of ultraviolet energy on the magnitude correction for various red shifts. If we multiply the observed solar energy distribution by factors corresponding to the data of the last column of Table 5, we can then repeat the integration which yielded K as a function of $d\lambda/\lambda$ in Table 4. The results of such an integration yield a value

of B^* of 3.33, which corresponds to a temperature for the solar spectrum (plus ultraviolet energy excess) of 5700°, an increase of 600° over the value obtained without the ultraviolet excess. The importance of the effect of an excess in the ultraviolet spectrum of late-type spirals requires further observation of the energy distribution, and apparently provides the only possibility of partly circumventing the difficulty raised by the low observed color temperatures of the nebulae. Hubble[16] has remarked that there is no obvious ultraviolet excess in the nebulae observed at Mount Wilson. Further, since there is no evidence for the existence of giant blue stars in ellipsoidal nebulae and in early-type spirals, there is little chance of raising the general mean color temperature of the nebulae. A possible observational test of the extreme difference in behavior of late-type spirals and ellipsoidal nebulae would be afforded by the relative frequency of spirals and ellipsoidals in distant clusters of extragalactic nebulae. The higher temperatures would result in smaller magnitude corrections arising from the red shifts for spirals than for ellipsoidals. The relative frequency of spirals should, therefore, increase among the fainter clusters of nebulae.

We may summarize the results briefly by stating that the spectral energy distribution of a nebula is roughly that of a black body over the range from λ 6500 to λ 3900, and that the temperature for the determination of the red-shift effect is less than 5250°. Unless the existence of an appreciable excess of ultraviolet energy can be proved, there is no available interpretation of the run of the present nebular counts with magnitude.

The observational material was obtained at the Yerkes and McDonald observatories, during my tenure as National Research Council Fellow, 1937–39. I am deeply indebted to Dr. Otto Struve and to members of the staff of these observatories for their kind cooperation.

McDONALD OBSERVATORY
AND
YERKES OBSERVATORY
August 1938

[16] *Ap. J.*, **84**, 541, 1936.

Fe III LINES IN STELLAR SPECTRA

P. SWINGS AND B. EDLÉN

ABSTRACT

A term analysis of the *Fe* III spectrum in the ultraviolet region enables the writers to predict *Fe* III lines which fall in the astronomically observable region. Several of them are present in B-type stars, both as absorption and as emission lines.

1. Owing to the high cosmic abundance of iron, the permitted lines of *Fe* III are to be expected in several astronomical spectra, namely, as absorption lines in early B-type stars and as emission lines in bright-line stars and novae, in the high chromosphere, etc. Attention has been drawn on several occasions to the possible importance of the *Fe* III forbidden transitions in connection with the spectra of novae, bright-line stars, nebulae, the solar corona, etc. In order to provide the required spectroscopic data for *Fe* III, which thus far have been lacking, we have attempted a term analysis of the *Fe* III spectrum, using vacuum-spark spectra in the region 2400–500 A, supplemented from 2400 to 1000 A by spectra of a spark in nitrogen. The analysis started from Bowen's classification[1] of the three important multiplets $a^5D - z^5P^o$, $a^7S - z^7P^o$, and $a^5S - z^5P^o$. At present the essential part of the septet and quintet terms lower than approximately 150,000 cm^{-1} has been established and some three hundred lines from 808 to 2150 A are classified. The analysis permits a prediction of the two multiplets of lowest excitation which fall in the astronomically observable region and presumably will give the most prominent of the permitted *Fe* III lines in astronomical spectra, namely, (*a*) $3d^5(^4P)4s^5P - 3d^5(^6S)4p^5P^o$ (from 4352 to 4431 A; excitation potential of the a^5P level = 8.22 e.v.); (*b*) $3d^5(^4D)4s^5D - 3d^5(^6S)4p^5P^o$ (from 5063 to 5194 A; excitation potential of the ^5D level = 8.62 e.v.).

The prediction and identification of these multiplets constitute the subject of this note.

2. The manner of connecting z^5P^o with a^5P and b^5D, as shown in Figure 1, involves lines with $\nu > 78{,}000$ cm^{-1}, giving an uncertainty

[1] *Phys. Rev.*, **52**, 1153, 1937.

of about 1 cm^{-1} in the absolute position of the predicted multiplets; on the other hand, the separations within each multiplet and between the two multiplets which were determined from transitions around 50,000 cm^{-1} were accurate to 0.1 cm^{-1}. This was sufficient to ascertain the identification of *Fe* III in γ Pegasi (B2), which has spectral characteristics suggesting the probable presence of *Fe* III absorption lines. Since the identification appeared to be certain be-

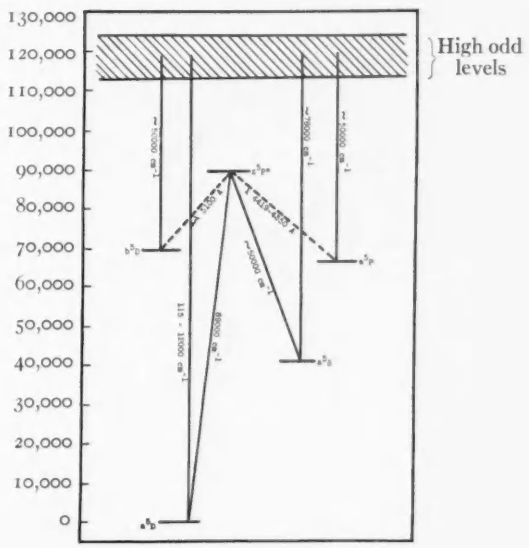

FIG. 1

yond any doubt, the connection by means of lines around 78,000 cm^{-1} was finally replaced by the assumption that the transition $a^5P_3 - z^5P_3^o$ has the value 4419.61 A, this being the mean of Struve's[2] and Kühlborn's[3] measured wave lengths in γ Peg; this meant a change of only 0.2 cm^{-1}. The wave lengths of the components of the two multiplets were calculated accordingly and may be found in Table 1.

3. The first multiplet falls in a region where we are provided with several good lists of wave lengths of absorption lines in B-type

[2] *Ap. J.*, **74**, 225, 1931.

[3] *Veröff. Babelsberg*, **12**, Heft 1, 1938.

stars, especially those of Struve and of Kühlborn. The identifications are summarized in Table 2.

The multiplet appears also in emission in Be stars. In BD + 11°4673, Merrill[4] measured an emission line at 4419.8 with an ab-

TABLE 1

$a^5P - z^5P^o$		λ	$b^5D - z^5P^o$		λ
1	1	4365.67	0	1	5063.52
1	2	4395.79	1	1	5073.79
2	1	4352.59	1	2	5114.53
2	2	4382.53	2	1	5086.78
2	3	4431.03	2	2	5127.72
3	2	4371.35	2	3	5194.26
3	3	4419.61	3	2	5127.38
.....	.....	.....	3	3	5193.91
.....	.....	.....	4	3	5156.10

TABLE 2

Predicted Laboratory Wave Length	Wave Length in Struve's List	Wave Length in Kühlborn's List	Intensity in γ Peg (B_2) (Kühlborn)	Remarks
4419.61	4419.62	4419.601	3	Observed also by Dawson,* Marshall,† Pillans,‡ possibly Struve and Dunham§
4382.53	4382.43	4382.52	2–3	.....
4365.67	.....	4365.66	1	Blend with *Ne* II (5.72)
4371.35	.....	4371.23	1–2	Blend with *A* II (1.36)
4431.03	4431.03	4431.08	2	Blend with *A* II (1.02) and possibly *S* II (1.02)
4352.59	4352.47	4352.48	1–2	Questionably attributed to *A* II (2.23) by Kühlborn, the principal contributor being unknown
4395.79	Blended with O II	blended	.....	.....

* *Pub. U. of Michigan Obs.*, **2**, 158, 1916.
† *Ibid.*, **5**, 137, 1934.
‡ *Ap. J.*, **80**, 51, 1934.
§ *Ibid.*, **77**, 321, 1933.

sorption component on the violet side.[5] Possibly the faint emission line measured by Lunt[6] at λ 4419.11 in η Carinae may be also due to

[4] *Ap. J.*, **69**, 330, 1929.

[5] A search for *Fe* III lines in "iron stars" would presumably give interesting results.

[6] *M.N.*, **79**, 621, 1919.

Fe III, though the wave length discrepancy seems somewhat large. In the list of emission lines of γ Cassiopeiae recently published by R. B. Baldwin,[7] the three lines at 4419.57 (intensity 1), 4382.63 (int. 0.3), and 4395.60 (int. 0) may be attributed to *Fe* III.

The second multiplet $b^5D - z^5P^o$ does not appear in Marshall's list[8] of lines of γ Ori (B2) and β Tau (B8) but may well be expected in suitable stars.

Dr. Struve has kindly called our attention to the following facts: λ 4419.61 is very conspicuous in P Cygni[9] both in emission and in absorption (int. 7 in absorption and 5 in emission); λ 4431 is also present as a fairly strong emission line (int. 4) and a weak absorption line (int. 3); λ 4352 is present in P Cygni as an emission line (int. 2); λ 4382.5 is also possibly present (int. 3 in emission and 1 in absorption); λ 4371 is probably present, although Struve identified it tentatively with *O* II 4369, in which case it gives a discordant radial velocity. There is also fairly good evidence that the second multiplet is present in P Cygni, giving an identification of the lines measured by Struve at roughly 5071 and 5125 A. The latter was measured both in emission and in absorption, the former only in absorption.[10] The density of the spectrograms used by Struve decreased very rapidly on the long wave-length side of λ 5154, and it is therefore not surprising that λ 5194 is not listed by him.

4. *Ionization potential of Fe III.*—The $(^6S)5s^7S$ term has been found at 119194.96 cm^{-1} above $(^6S)4s^7S$. This gives an ionization energy of about 26.7 e.v. from the $4s^7S$ level. No intercombination between quintets and septets has been found as yet, but it seems safe to assume that the $4s^7S$ is somewhere around 29,500 cm^{-1} above the ground level, which gives an ionization energy of approximately 30.3 e.v. from the ground level a^5D.

The analysis is being continued with the hope of discussing the forbidden transitions.

DEPARTMENT OF ASTROPHYSICS, UNIVERSITY OF LIÉGE
AND
DEPARTMENT OF PHYSICS, UNIVERSITY OF UPSALA
July 1938

[7] *Ap. J.*, **87**, 573, 1938.
[8] *Ibid.*, **82**, 97, 1935.
[9] *Ibid.*, **81**, 73, 1935.
[10] *Op. cit.*, p. 95.

NOTES

RECENT CHANGES IN THE SPECTRUM OF PLEIONE

ABSTRACT

Spectrograms taken in October and November, 1938, show the return of hydrogen emission in the spectrum of Pleione, after an absence of 32 years. Strong sharp absorption bisects the emission, and numerous faint sharp enhanced metallic absorption lines are present.

The disappearance of the hydrogen emission lines from the spectrum of Pleione[1] in 1906 was the first recorded instance of its kind. The observations bearing on it have been summarized by the late R. H. Curtiss.[2]

Since 1912, occasional spectrograms of this star have been taken at the Michigan Observatory to record the possible return of the bright lines. All such plates up to 1936, inclusive, show the hydrogen lines as very strong absorption with widths of 3–4 angstroms in their more intense central portions and with wider faint wings, doubtless due to Stark broadening. $H\alpha$ remained a strong absorption line until 1935, inclusive, and was not observed in 1936. No plates of Pleione were secured here in 1937.

A spectrogram taken October 28, 1938, by W. C. Rufus and R. C. Williams shows $H\alpha$ as a conspicuous emission line with a fine central reversal. Details in the photographic region are shown better by exposures on Eastman 33 emulsion, taken October 29 and November 1 and 9. The lines $H\beta$ and $H\gamma$ are filled up with emission approximately as strong as the neighboring continuum and about 7.5 A wide at $H\beta$. Each emission line is bisected by very strong and very sharp absorption. Similar strong and narrow absorption cores are seen as far out in the Balmer series as $H\eta$, but with progressive weakening of the emission, the wings of the underlying diffuse absorption become noticeable at $H\epsilon$ and prominent at $H\eta$ and at higher members of the series.

[1] 28 Tauri, 1900: α $3^h\ 43^m3$; $\delta+23°51'$; mag. 5.18; Spec. B8ev.

[2] *Pub. Obs. U. Michigan*, **3**, 19, 1923.

Throughout the spectrum there are many weak, narrow lines of ionized metals. *Fe* II is abundantly represented, *Ti* II shows most of its stronger lines and some lines of *Sc* II, *Cr* II, and *Ni* II, and perhaps lines of *V* II are present. The *He* I lines λ 4472 and λ 4026 are complicated by blending, but λ 3819 is conspicuous and is wider than the metallic lines. The lines of *Si* II and *Mg* II 4481 are possibly (but not conspicuously) wider than those of other metals. The present spectrum of Pleione is thus similar in its general appearance to that of ε Capricorni.

DEAN B. MCLAUGHLIN

THE OBSERVATORY
UNIVERSITY OF MICHIGAN
November 10, 1938

SOME CHANGES IN THE SPECTRA OF THE PLEIADES

ABSTRACT

Hydrogen emission is again present in the spectrum of Pleione (HD 23862) after an absence of 32 years. Sharp metallic absorption lines are also now present. Hydrogen emission in Electra appears to have faded.

Spectrograms of Pleione (HD 23862) taken October 26.250, October 28.247, and November 1.284, 1938, U.T., show *Hα* in emission, estimated 1.5 times as strong as the near-by continuous spectrum. Hydrogen emission has not been observable in this star for 32 years. Sharp absorption lines (*Fe* II) constitute a major change in the appearance of Pleione's spectrum.

Hα emission in Electra (HD 23302) has become very faint or has vanished; but since this emission has never been very strong, spectrophotometric measures will be made to test the reality of the suspected variation. A visual comparison of an O-type (blue-sensitive) plate taken in 1935 and an F-type (red-sensitive) plate of November, 1938, does not show any obvious change in the blue-violet region of the spectrum.

ORREN MOHLER

COOK OBSERVATORY
November 10, 1938

REVIEWS

Through Science to Philosophy. By HERBERT DINGLE. Pp. vi+363. Figs. 18. 14 × 22 cm. Oxford: Oxford University Press, 1937. $6.25.

For the first time in history the population in civilized countries consists largely of educated people, and science holds the highest place in popular interest. But, alas, no sooner has this come about than "knowledge of all kinds begins to assume a cloak of absurdity" which supports mysticism and leads the public to believe that modern science is utterly beyond comprehension. To help remedy this situation and restore to the common man the proper confidence in his own judgment, the author attempts to work out a rational scheme of thought in which classical and modern physics appear intelligible, and as products of a continuous rational activity. The result of his efforts is a very vigorous and stimulating book which should be read by everyone interested in physical science.

Dingle contrasts the older conception of science as the study of nature with recent statements by Bohr and Einstein according to which the task of science is to extend and correlate experience. He adopts the latter view as the more fundamental but greatly limits the scope of his work by considering only the correlation and not the extension of experience. Since he insists on defining not only such concepts as "nature" and "external world" but also "other normal people" in terms of the contents of his own consciousness, he must carry his analysis down to the solipsistic level. He defines philosophy as "the rational correlation of the whole of experience." As indicated by the title of the book, he believes that it will be reached most surely through the expansion of the sciences.

The development of a solipsistic description in which the common-sense duality of mind and matter is replaced by that of reason and experience takes up nearly half of the book. My field of consciousness consists of the memories of all my past experiences, and reason operates to reduce them to order. The various steps in this process are illustrated by very apt diagrams. While the process of rational correlation is discussed in great detail, no attempt is made to analyze the rules of logic.

According to Dingle, science and common sense represent two independent schemes of rationalization created for different purposes. Common sense associates unlike elementary experiences to form "physical

objects," whereas in science elementary experiences of the same kind are correlated by such concepts as "motion," "light," etc. This difference between science and common sense has existed ever since the days of Galileo, although we have only recently become aware of it. "For 300 years the palace of science has been built by men almost completely unaware of what they were doing; like the British empire, it has been created in absent-mindedness." Dingle criticizes the "physical object mania"; the supposed dilemma "that we can examine the world only with parts of that same world, so that those parts themselves necessarily escape observation" he denounces as "the complete delusion." In the opinion of the reviewer, Dingle oversimplifies the relation between common sense and science. While science has gone beyond common sense from the very beginning, it seems indisputable that the gap has gradually widened. Moreover, the two schemes cannot be independent; for it is impossible to describe the measuring instruments and operations which define the concepts of modern physics without the aid of the thing concept of common sense.

It is an essential characteristic of scientific knowledge that it is valid for all normal people and that its advance depends upon the co-operation of many scientists. Hence, a chapter is devoted to describing intercourse between "myself" and "other people" in solipsistic terms. The last chapter of Part I deals with the necessary adaptation of our language to the new epistemological viewpoint.

The second part of the book begins with a chapter entitled "Knowledge, Truth, and 'Unobservables,' " in which the author briefly outlines his theory of knowledge. The next two chapters on "Subjective and Physical Time" and "The 'Measurement' of Time and the Running-Down of the Universe" deal with the important and difficult problems connected with the concept of time. Dingle concludes that

> physical time is an extension created by reason as part of a general structure of conceptions. It is a capacity for arranging in sequence events which are postulated in order to knit together experiences in a molecule by the one-way relation known as the cause-and-effect relation. In the network thus formed a rationally created event is both an effect and a cause, but experience is only an effect; and both this distinction and the cause-to-effect direction of time are maintained by placing rationally created events elsewhere in another extension called space in which experiences are always here, and postulating a communicating agent which travels in only one direction in time and only from cause to effect.

We cannot measure time as we can measure space; for no time standard can be preserved.

> The process known as the measurement of time . . . . consists in choosing some . . . . temporal sequence of events between successive members of which there is also an interval of some non-temporal measurable quantity, and then defining the time interval between any two events as proportional to the corresponding interval of this measurable quantity.

It is arbitrary that we let the laws of thermodynamics rather than those of mechanics exhibit the going-on of time. At present, the order of events in nature gives no evidence at all concerning the origin or destiny of the universe, or even of the sun. Milne's and Eddington's theories of time are discussed and rejected. Since causality is inseparably associated with time, the next chapter is devoted to the study of this category. It is pointed out that while causality has a tendency to fade out of science, it is required again when the completely described world is connected up with experience.

In the thirteenth chapter Dingle discusses the general ideas and paradoxes of the quantum theory. He shows that most of the difficulties arose because the electron was regarded as a physical object. Since he can give no satisfactory definition of the electron, he considers the quantum theory as essentially unfinished. Although Dingle's epistemological viewpoint is for all practical purposes equivalent to that of Bohr and Heisenberg, he does not mention their solution of the quantum-theoretical paradoxes which was achieved by redefining the particle concept in such a manner that it applies on the atomic as well as on the macroscopic level.

The next chapter, which is an adaptation of part of the author's 1936 Joseph Henry lecture, gives a very readable explanation of what cosmologists mean by such terms as "the universe" and "curved space." The book ends with a chapter entitled "Remarks on Current Philosophies," with the subtitles "Logical Positivism," "Sir Arthur Eddington and Solipsism," and "Professor Whitehead, Science and Poetry." The discussion of the logical positivists is not very adequate and tends to conceal the kinship between the author's and their viewpoints. With Dingle's criticism of Eddington most physicists and philosophers will agree. The remarks on Whitehead's position and the relation of science and poetry form a very fitting finale to the book.

When an astrophysicist makes such a bold and ambitious venture into the theory of knowledge, he necessarily lays himself open to criticism from many sides. The layman, who has only secondhand acquaintance with science, can hardly find the solipsistic description natural. Many physicists, while admitting the importance of the solipsistic viewpoint, will feel that too much space has been devoted to describing this position and too little

space to the clarification of physical problems. On the other hand, philosophers will find Dingle's treatment of solipsism sketchy and, in places, somewhat crude. The reviewer would have welcomed a greater emphasis upon deduction and a clearer recognition of the fact that induction is not a perfectly logical process. He feels also that Dingle gives too little attention to the work of contemporary Continental physicists and epistemologists and is too concerned with Eddington's epistemological sins (which are bad enough). However, if that had not been the case, this very interesting and valuable book might not have been written.

J. Rud Nielsen

University of Oklahoma

INDEX TO VOLUME 88

SUBJECTS

AUTHORS

DEC 23 1938

VOLUME 88 NUMBER 5

THE ASTROPHYSICAL JOURNAL

AN INTERNATIONAL REVIEW OF SPECTROSCOPY AND ASTRONOMICAL PHYSICS

Founded in 1895 by GEORGE E. HALE *and* JAMES E. KEELER

Edited by

HENRY G. GALE
Ryerson Physical Laboratory of the University of Chicago

FREDERICK H. SEARES
Mount Wilson Observatory of the Carnegie Institution of Washington

OTTO STRUVE
Yerkes Observatory of the University of Chicago

DECEMBER 1938

THE UNIVERSITY OF CHICAGO PRESS
CHICAGO, ILLINOIS, U.S.A.

December 1938 Vol. 88, No. 5

THE ASTROPHYSICAL JOURNAL

AN INTERNATIONAL REVIEW OF SPECTROSCOPY AND ASTRONOMICAL PHYSICS

Edited by

HENRY G. GALE
Ryerson Physical Laboratory of the University of Chicago

FREDERICK H. SEARES
Mount Wilson Observatory of the Carnegie Institution of Washington

OTTO STRUVE
Yerkes Observatory of the University of Chicago

WITH THE COLLABORATION OF

WALTER S. ADAMS, Mount Wilson Observatory
JOSEPH S. AMES, Johns Hopkins University
HENRY CREW, Northwestern University
CHARLES FABRY, Université de Paris
ALFRED FOWLER, Imperial College, London
EDWIN HUBBLE, Mount Wilson Observatory
HEINRICH KAYSER, Universität Bonn
ROBERT A. MILLIKAN, Institute of Technology, Pasadena
HUGH F. NEWALL, Cambridge University
FRIEDRICH PASCHEN, Reichsanstalt, Charlottenburg
HENRY N. RUSSELL, Princeton University
FRANK SCHLESINGER, Yale Observatory
HARLOW SHAPLEY, Harvard College Observatory

Former Editors:

GEORGE E. HALE JAMES E. KEELER EDWIN B. FROST

The Astrophysical Journal is published by the University of Chicago at the University of Chicago Press, 5750 Ellis Avenue, Chicago, Illinois, during each month except February and August. ¶The subscription price is $10.00 a year; the price of single copies is $1.50. Orders for service of less than a half-year will be charged at the single-copy rate. ¶Postage is prepaid by the publishers on all orders from the United States, Mexico, Cuba, Puerto Rico, Panama Canal Zone, Republic of Panama, Dominican Republic, Canary Islands, El Salvador, Argentina, Bolivia, Brazil, Colombia, Chile, Costa Rica, Ecuador, Guatemala, Honduras, Nicaragua, Peru, Hayti, Uruguay, Paraguay, Hawaiian Islands, Philippine Islands, Guam, Samoan Islands, Balearic Islands, Spain, and Venezuela. ¶Postage is charged extra as follows: for Canada and Newfoundland, 30 cents on annual subscriptions (total $10.30); on single copies, 3 cents (total $1.53); for all other countries in the Postal Union, 80 cents on annual subscriptions (total $10.80), on single copies, 8 cents (total $1.58). ¶Patrons are requested to make all remittances payable to The University of Chicago Press, in postal or express money orders or bank drafts.

The following are authorized agents:

For the British Empire, except North America, India, and Australasia: The Cambridge University Press, Fetter Lane, London, E.C. 4. Prices of yearly subscriptions and of single copies may be had on application.

For Japan: The Maruzen Company, Ltd., Tokyo.

For China: The Commercial Press, Ltd., 211 Honan Road, Shanghai. Yearly subscriptions, $10.00; single copies, $1.50, or their equivalents in Chinese money. Postage extra, on yearly subscriptions 80 cents, on single copies 8 cents.

Claims for missing numbers should be made within the month following the regular month of publication. The publishers expect to supply missing numbers free only when losses have been sustained in transit, and when the reserve stock will permit.

Business correspondence should be addressed to The University of Chicago Press, Chicago, Illinois.

Communications for the editors and manuscripts should be addressed to: Otto Struve, Editor of THE ASTROPHYSICAL JOURNAL, Yerkes Observatory, Williams Bay, Wisconsin.

The cable address is "Observatory, Williamsbay, Wisconsin."

The articles in this journal are indexed in the *International Index to Periodicals*, New York, N.Y.

Applications for permission to quote from this journal should be addressed to The University of Chicago Press, and will be freely granted.

Entered as second-class matter, January 17, 1895, at the Post-Office, Chicago, Ill., under the act of March 3, 1879.
Acceptance for mailing at special rate of postage provided for in Section 1103, Act of October 3, 1917, authorized on July 15, 1918.

PRINTED IN THE U.S.A.

AN INTRODUCTION TO THE STUDY OF STELLAR STRUCTURE

By S. CHANDRASEKHAR

In this monograph the subject of stellar interiors is treated in a deductive manner, the necessary physical theories and mathematical methods being fully explained. The book includes accounts of the foundations of thermodynamics, the theory of radiation, the quantum theory of a perfect gas, and also a discussion of the elements of nuclear physics. The mathematical theory of the equilibrium of gaseous spheres is exhaustively treated. The applications of the theory to the elucidation of the structure of the stars is also considered. Further, two special chapters deal with the physical properties of highly dense matter and the theory of the white dwarfs.

The monograph should be of interest to both physicists and astronomers. It may be used as an advanced text-book in theoretical astrophysics, and it is also intended as a standard work on the theory of stellar interiors.

Ready in December, $10.00—In the series, Astrophysical Monographs

THE UNIVERSITY OF CHICAGO PRESS

THE OBSERVATORY

A Monthly Review of Astronomy, Founded 1877

Contains full Reports (including the speakers' accounts of their work and the discussions which follow) of the Meetings of the Royal Astronomical Society and of the Meetings for Geophysical Discussion: Articles: Reviews of important astronomical books: Correspondence on topics of interest: Notes on current discoveries and research, etc.

Annual Subscription: 20/– for 12 Numbers.

The Observatory, founded in 1877 by Sir Wm. Christie, Astronomer Royal, has been edited in the past by W. H. M. Christie, E. W. Maunder, A. M. W. Downing, T. Lewis, H. H. Turner, A. A. Common, H. P. Hollis, S. Chapman, A. S. Eddington, H. Spencer Jones, F. J. M. Stratton, J. Jackson, W. M. H. Greaves, J. A. Carroll, W. H. Steavenson, R. O. Redman, and H. W. Newton.

Address of Editors: Royal Observatory, Greenwich, England.

21 TRANSPARENCIES (14X17) FROM YERKES OBSERVATORY AT UNUSUAL PRICES:

PROFESSOR E. E. BARNARD made many of these from photographs obtained by him with the Bruce photographic telescope of Yerkes.

$3.00 each, without ground glass

$4.00 each, with ground glass

POSTAGE AND INSURANCE EXTRA

Positives, 14×17 inches, enlarged from negatives made with the Bruce photographic telescope of the Yerkes Observatory. These positives are not covered.

	α	δ		REMARKS
1	2^h12^m	+57°	Double cluster of Perseus	Dense
1	5 45	+32	Region of Messier 37, in Aurigae	Good; medium density
1	6 2	+24	Region of Messier 35, in Gemini	Dense
1	6 23	+22	In Gemini—M35 and NGC 2175; also trail of Comet 1905 III (Giacobini)	Dense; fainter nebulosity lost
1	16 20	−23	Region of Rho Ophiuchi	Medium density
1	16 55	−32	In Scorpius, near Messier 62; area of dark markings	Thin
1	17 10	−27	In Ophiuchus and Scorpius	Very good; a little dark
1	17 35	−22	Region of 58 Ophiuchi	Good; medium density
1	17 56	−28	In Sagittarius	Much enlarged
1	17 56	−28	In Sagittarius	Rather soft contrast
1	17 56	−30	In Sagittarius	Medium density
1	18 10	−20	Small star cloud in Sagittarius	Excellent; medium density
1	18 20	−23	In Sagittarius; area dark markings	Medium density; soft contrast
1	18 20	−25	In Sagittarius; area dark markings	Good; medium density
1	18 20	−15	In Aquila and Sagittarius	Medium density
1	18 30	−11	In Aquila and Sagittarius	Medium density
1	18 40	− 6	Star Cloud in Scutum	Much enlarged; not best quality
1	18 45	− 6	Star Cloud in Scutum	Good; medium density
1	21 35	+57	In Cepheus	Thin, soft; much enlarged
1	21 36	+56	In Cepheus	Good; greatly enlarged
1	21 36	+50	In Cepheus	Dense; greatly enlarged

For complete information on Yerkes material and catalogue, write to:

THE UNIVERSITY OF CHICAGO PRESS

5750 ELLIS AVENUE, CHICAGO, ILLINOIS